$s(t)$ to maximize d^2. The solution follows directly from our earlier signal design results (p. 302). We can express d^2 in terms of the channel eigenvalues and eigenfunctions

$$d^2 = \frac{2}{N_0} \sum_{i=1}^{\infty} \lambda_i^{\text{ch}} s_i^2, \tag{346}$$

where

$$s_i \triangleq \int_a^b \sqrt{E}\, s(u)\, \phi_i(u)\, du \tag{347}$$

and λ_i^{ch} and $\phi_i(u)$ correspond to the kernel $Q_{\text{ch}}(u, v)$. To maximize d^2 we choose

$$s_1 = \sqrt{E},$$

and

$$s_i = 0, \qquad i \neq 1, \tag{348}$$

because λ_1^{ch} is defined as the largest eigenvalue of the channel kernel $Q_{\text{ch}}(u, v)$. Some typical channels and their optimum signals are developed in the problems.

When we try to communicate sequences of signals over channels with memory, another problem arises. Looking at the basic communications system in Fig. 4.1, we see that inside the basic interval $0 \leq t \leq T$ there is interference due to noise and the sequence of signals corresponding to previous data. This second interference is referred to as the intersymbol interference and it turns out to be the major disturbance in many systems of interest. We shall study effective methods of combatting intersymbol interference in Chapter II.4.

4.4 SIGNALS WITH UNWANTED PARAMETERS: THE COMPOSITE HYPOTHESIS PROBLEM

Up to this point in Chapter 4 we have assumed that the signals of concern were completely known. The only uncertainty was caused by the additive noise. As we pointed out at the beginning of this chapter, in many physical problems of interest this assumption is not realistic. One example occurs in the radar problem. The transmitted signal is a high frequency pulse that acquires a random phase angle (and perhaps a random amplitude) when it is reflected from the target. Another example arises in the communications problem in which there is an uncertainty in the oscillator phase. Both problems are characterized by the presence of an unwanted parameter.

Unwanted parameters appear in both detection and estimation problems. Because of the inherent similarities, it is adequate to confine our present discussion to the detection problem. In particular, we shall discuss general binary detection. In this case the received signals under the two hypotheses are

$$\begin{aligned} r(t) &= s_1(t, \boldsymbol{\theta}) + n(t), \qquad T_i \le t \le T_f : H_1, \\ r(t) &= s_0(t, \boldsymbol{\theta}) + n(t), \qquad T_i \le t \le T_f : H_0. \end{aligned} \tag{349}$$

The vector $\boldsymbol{\theta}$ denotes an unwanted vector parameter. The functions $s_0(t, \boldsymbol{\theta})$ and $s_1(t, \boldsymbol{\theta})$ are conditionally deterministic (i.e., if the value of $\boldsymbol{\theta}$ were known, the values of $s_0(t, \boldsymbol{\theta})$ and $s_1(t, \boldsymbol{\theta})$ would be known for all t in the observation interval). We see that this problem is just the waveform counterpart to the classical composite hypothesis testing problem discussed in Section 2.5. As we pointed out in that section, three types of situations can develop:

1. $\boldsymbol{\theta}$ is a random variable with a known a priori density;
2. $\boldsymbol{\theta}$ is a random variable with an unknown a priori density;
3. $\boldsymbol{\theta}$ is a nonrandom variable.

We shall confine our discussion here to the first situation. At the end of the section we comment briefly on the other two. The reason for this choice is that the two physical problems encountered most frequently in practice can be modeled by the first case. We discuss them in detail in Sections 4.4.1 and 4.4.2, respectively.

The technique for solving problems in the first category is straightforward. We choose a finite set of observables and denote them by the K-dimensional vector $\mathbf{r}$. We construct the likelihood ratio and then let $K \to \infty$.

$$\Lambda[r(t)] \triangleq \lim_{K \to \infty} \frac{p_{\mathbf{r}|H_1}(\mathbf{R}|H_1)}{p_{\mathbf{r}|H_0}(\mathbf{R}|H_0)}. \tag{350}$$

The only new feature is finding $p_{\mathbf{r}|H_1}(\mathbf{R}|H_1)$ and $p_{\mathbf{r}|H_0}(\mathbf{R}|H_0)$ in the presence of $\boldsymbol{\theta}$. If $\boldsymbol{\theta}$ were known, we should then have a familiar problem. Thus an obvious approach is to write

$$p_{\mathbf{r}|H_1}(\mathbf{R}|H_1) = \int_{\chi_{\boldsymbol{\theta}}} p_{\mathbf{r}|\boldsymbol{\theta},H_1}(\mathbf{R}|\boldsymbol{\theta}, H_1)\, p_{\boldsymbol{\theta}|H_1}(\boldsymbol{\theta}|H_1)\, d\boldsymbol{\theta}, \tag{351}$$

and

$$p_{\mathbf{r}|H_0}(\mathbf{R}|H_0) = \int_{\chi_{\boldsymbol{\theta}}} p_{\mathbf{r}|\boldsymbol{\theta},H_0}(\mathbf{R}|\boldsymbol{\theta}, H_0)\, p_{\boldsymbol{\theta}|H_0}(\boldsymbol{\theta}|H_0)\, d\boldsymbol{\theta}. \tag{352}$$

Substituting (351) and (352) into (350) gives the likelihood ratio. The tractability of the procedure depends on the form of the functions to be integrated. In the next two sections we consider two physical problems in which the procedure leads to easily interpretable results.

4.4.1 Random Phase Angles

In this section we look at several physical problems in which the uncertainty in the received signal is due to a random phase angle. The first problem of interest is a radar problem. The transmitted signal is a bandpass waveform which may be both amplitude- and phase-modulated. We can write the transmitted waveform as

$$s_t(t) = \begin{cases} \sqrt{2E_t}\, f(t) \cos\,[\omega_c t + \phi(t)], & 0 \le t \le T, \\ 0, & \text{elsewhere.} \end{cases} \tag{353}$$

Two typical waveforms are shown in Fig. 4.50. The function $f(t)$ corresponds to the envelope and is normalized so that the transmitted energy is E_t. The function $\phi(t)$ corresponds to a phase modulation. Both functions are low frequency in comparison to ω_c.

For the present we assume that we simply want to decide whether a target is present at a particular range. If a target is present, the signal will be reflected. In the simplest case of a fixed point target, the received waveform will be an attenuated version of the transmitted waveform with a random phase angle added to the carrier. In addition, there is an additive white noise component $w(t)$ at the receiver whether the target is present or

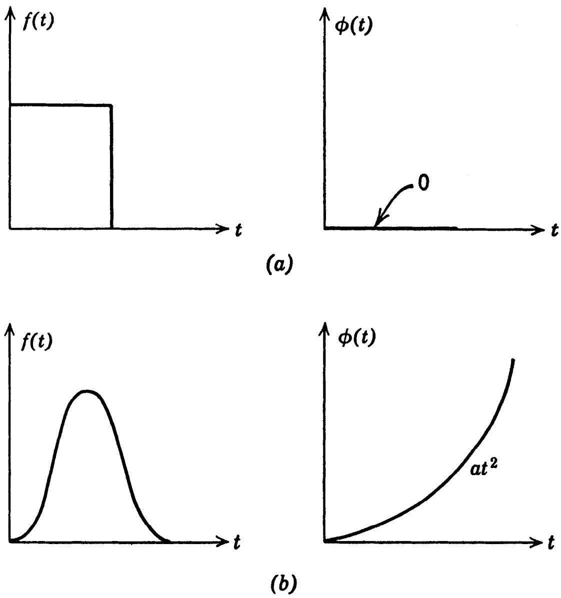

Fig. 4.50 Typical envelope and phase functions.

not. If we define H_1 as the hypothesis that the target is present and H_0 as the hypothesis that the target is absent, the following detection problem results:

$$\begin{aligned} H_1\!:r(t) &= \sqrt{2E_t}\, f(t-\tau)\cos(\omega_c(t-\tau)+\phi(t-\tau)+\theta) \\ &\qquad\qquad + w(t), \qquad \tau \le t \le \tau + T, \\ &= \qquad\qquad\quad w(t), \qquad T_i \le t < \tau,\ \tau + T < t \le T_f, \\ &\triangleq s_r(t-\tau,\theta) + w(t), \qquad T_i \le t \le T_f. \end{aligned} \tag{354a}$$

$$H_0\!:r(t) = w(t); \qquad T_i \le t \le T_f. \tag{354b}$$

Because the noise is white, we need only observe over the interval $\tau \le t \le \tau + T$. Under the assumption that we are interested only in a particular τ, the model is the same if we let $\tau = 0$. Thus we need only consider the problem

$$H_1\!:r(t) = s_r(t,\theta) + w(t), \qquad 0 \le t \le T, \tag{355a}$$

$$H_0\!:r(t) = \qquad\quad w(t), \qquad 0 \le t \le T. \tag{355b}$$

Here we have a simple binary detection problem in which the unknown parameter occurs only on one hypothesis. Before solving it we indicate how a similar problem can arise in the communications context.

In a simple on-off communication system we send a signal when the source output is "one" and nothing when the source output is "zero". The transmitted signals on the two hypotheses are

$$\begin{aligned} H_1\!:s_t(t) &= \sqrt{2E_t}\, f(t)\cos(\omega_c t + \phi(t) + \theta_a), \qquad 0 \le t \le T, \\ H_0\!:s_t(t) &= 0, \qquad\qquad\qquad\qquad\qquad\qquad\quad 0 \le t \le T. \end{aligned} \tag{356}$$

Frequently, we try to indicate to the receiver what θ_a is. One method of doing this is to send an auxiliary signal that contains information about θ_a. If this signal were transmitted through a noise-free channel, the receiver would know θ_a exactly and the problem would reduce to the known signal problem. More frequently the auxiliary signal is corrupted by noise and the receiver operates on the noise-corrupted auxiliary signal and tries to estimate θ_a. We denote this estimate by $\hat{\theta}_a$. A block diagram is shown in Fig. 4.51. We discuss the detailed operation of the lower box in Chapter II.2. Now, if the estimate $\hat{\theta}_a$ equals θ_a, the problem is familiar. If they are unequal, the uncertainty is contained in the difference $\theta = \theta_a - \hat{\theta}_a$, which is a random variable. Therefore we may consider the problem:

$$H_1\!:r(t) = \sqrt{2E_r}\, f(t)\cos(\omega_c t + \phi(t) + \theta) + w(t), \qquad 0 \le t \le T, \tag{357}$$

$$H_0\!:r(t) = w(t), \qquad 0 \le t \le T, \tag{358}$$

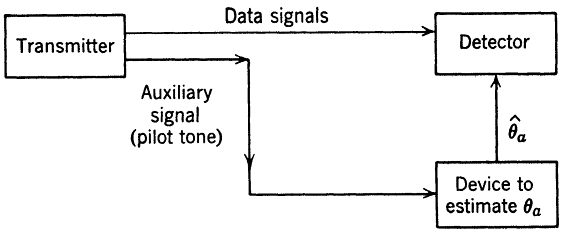

Fig. 4.51 A phase estimation system.

where E_r is the actual received signal energy and θ is the phase measurement error. We see that the radar and communication problems lead to the same mathematical model.

The procedure for finding the likelihood ratio was indicated at the beginning of Section 4.4. In this particular case the model is so familiar (see (23)) that we can write down the form for $K \to \infty$ immediately. The resulting likelihood ratio is

$$\Lambda[r(t)] = \int_{-\pi}^{\pi} p_\theta(\theta)\, d\theta \exp\left[+\frac{2}{N_0}\int_0^T r(t)\, s_r(t, \theta)\, dt - \frac{1}{N_0}\int_0^T s_r^2(t, \theta)\, dt\right], \tag{359}$$

where we assume the range of θ is $[-\pi, \pi]$. The last integral corresponds to the received energy. In most cases of interest it will not be a function of the phase so we incorporate it in the threshold. To evaluate the other integral, we expand the cosine term in (357),

$$\cos[\omega_c t + \phi(t) + \theta] = \cos[\omega_c t + \phi(t)]\cos\theta - \sin[\omega_c t + \phi(t)]\sin\theta, \tag{360}$$

and define

$$L_c \triangleq \int_0^T \sqrt{2}\, r(t)\, f(t) \cos[\omega_c t + \phi(t)]\, dt, \tag{361}$$

and

$$L_s \triangleq \int_0^T \sqrt{2}\, r(t)\, f(t) \sin[\omega_c t + \phi(t)]\, dt. \tag{362}$$

Thus the integral of interest is

$$\Lambda'[r(t)] = \int_{-\pi}^{\pi} p_\theta(\theta)\, d\theta \exp\left[\frac{2\sqrt{E_r}}{N_0}(L_c\cos\theta - L_s\sin\theta)\right]. \tag{363}$$

To proceed we must specify $p_\theta(\theta)$. Instead of choosing a particular density, we specify a family of densities indexed by a single parameter. We want to choose a family that will enable us to model as many cases of interest as

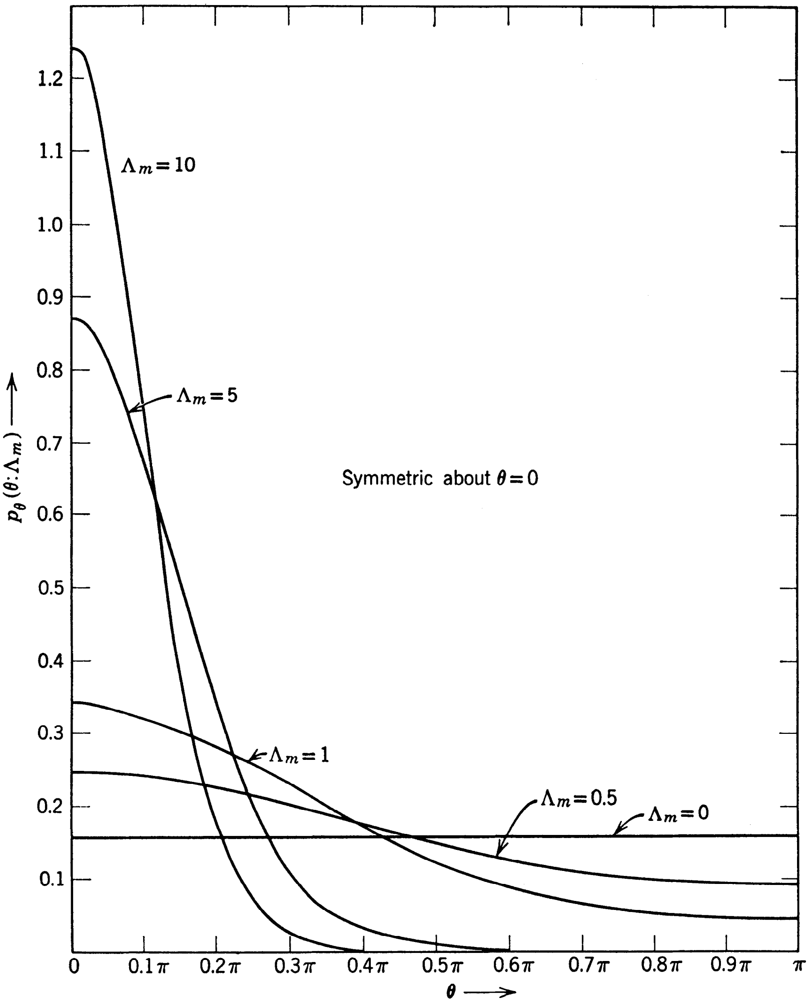

Fig. 4.52 Family of probability densities for the phase angle.

possible. A family that will turn out to be useful is given in (364) and shown in Fig. 4.52†:

$$p_\theta(\theta:\Lambda_m) = \frac{\exp\,[\Lambda_m \cos\theta]}{2\pi\, I_0(\Lambda_m)}; \qquad -\pi \leq \theta \leq \pi. \tag{364}$$

The function $I_0(\Lambda_m)$ is a modified Bessel function of the first kind which is included so that the density will integrate to unity. For the present Λ_m

† This density was first used for this application by Viterbi [44].

can be regarded simply as a parameter that controls the spread of the density. When we study phase estimators in Chapter II.2, we shall find that it has an important physical significance.

Looking at Fig. 4.52, we see that for $\Lambda_m = 0$

$$p_\theta(\theta) = \frac{1}{2\pi}, \qquad -\pi \leq \theta \leq \pi. \tag{365}$$

This is the logical density for the radar problem. As Λ_m increases, the density becomes more peaked. Finally, as $\Lambda_m \to \infty$, we approach the known signal case. Thus by varying Λ_m we can move continuously from the known signal problem through the intermediate case, in which there is some information about the phase, to the other extreme, the uniform phase problem.

Substituting (364) into (363), we have

$$\Lambda'[r(t)] = \int_{-\pi}^{\pi} \frac{1}{2\pi\, I_0(\Lambda_m)} \exp\left[\left(\Lambda_m + \frac{2\sqrt{E_r}}{N_0} L_c\right)\cos\theta - \frac{2\sqrt{E_r}}{N_0} L_s \sin\theta\right] d\theta. \tag{366}$$

This is a standard integral (e.g., [45]). Thus

$$\Lambda'[r(t)] = \frac{1}{I_0(\Lambda_m)} I_0\left\{\left[\left(\Lambda_m + \frac{2\sqrt{E_r}}{N_0} L_c\right)^2 + \left(\frac{2\sqrt{E_r}}{N_0} L_s\right)^2\right]^{1/2}\right\}. \tag{367}$$

Substituting (367) into (359), incorporating the threshold, and taking the logarithm, we obtain

$$\ln I_0\left\{\left[\left(\Lambda_m + \frac{2\sqrt{E_r}\,L_c}{N_0}\right)^2 + \left(\frac{2\sqrt{E_r}\,L_s}{N_0}\right)^2\right]^{1/2}\right\} \underset{H_0}{\overset{H_1}{\gtrless}} \ln\eta + \frac{E_r}{N_0} + \ln I_0(\Lambda_m). \tag{368}$$

The formation of the test statistic is straightforward (Fig. 4.53). The function $I_0(\cdot)$ is shown in Fig. 4.54. For large x

$$I_0(x) \simeq \frac{e^x}{\sqrt{2\pi x}}, \qquad x \gg 1, \tag{369}$$

whereas for small x

$$I_0(x) \simeq 1 + \frac{x^2}{4}, \qquad x \ll 1, \tag{370a}$$

and

$$\ln I_0(x) \simeq \frac{x^2}{4}, \qquad x \ll 1. \tag{370b}$$

Observe that because $\ln I_0(x)$ is monotone we can remove it by modifying

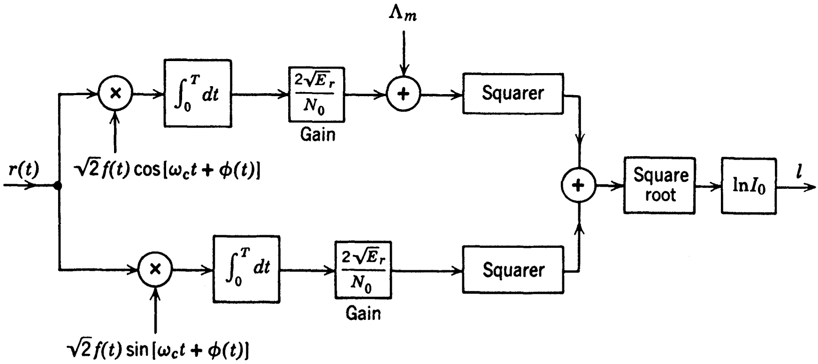

Fig. 4.53 Optimum receiver: random phase angle

the threshold. Thus two tests equivalent to (368) are

$$\left(L_c + \frac{N_0\Lambda_m}{2\sqrt{E_r}}\right)^2 + L_s^2 \underset{H_0}{\overset{H_1}{\gtrless}} \gamma \tag{371a}$$

and

$$\left(\frac{2\sqrt{E_r}}{N_0}\right)^2(L_c^2 + L_s^2) + 2\Lambda_m \frac{2\sqrt{E_r}}{N_0} L_c \underset{H_0}{\overset{H_1}{\gtrless}} \gamma'. \tag{371b}$$

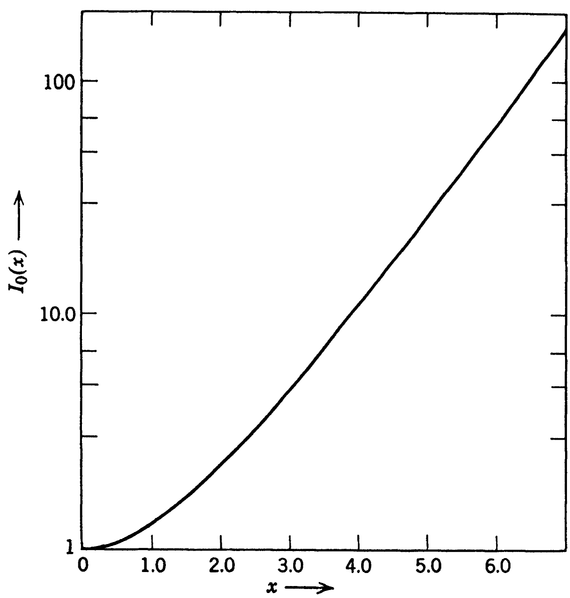

Fig. 4.54 Plot of $I_0(x)$.

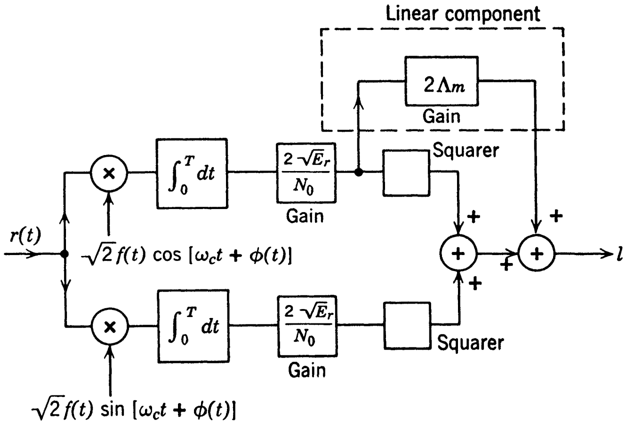

Fig. 4.55 Alternate realization of optimum receiver.

Redrawing the receiver structure as shown in Fig. 4.55, we see that the optimum receiver consists of a linear component and a square-law component.

Looking at (371*a*), we see that the region in the L_c, L_s plane corresponding to the decision H_0 is the interior of a circle centered at $(-N_0\Lambda_m/2\sqrt{E_r}, 0)$ with radius $\gamma^{1/2}$. We denote this region as Ω_0. The probability density of L_c and L_s under H_0 is a circularly symmetric Gaussian density centered at the origin. Therefore, if γ is fixed and Λ_m is allowed to increase, Ω_0 will move to the left and the probability of being in it on H_0 will decrease. Thus, to maintain a constant P_F we increase γ as Λ_m is increased. Several decision regions are shown in Fig. 4.56. In the limit, as $\Lambda_m \to \infty$, the decision boundary approaches a straight line and we have the familiar known signal problem of Section 4.2. The probability density on H_1 depends on θ. A typical case is shown in the figure. We evaluate P_F and P_D for some interesting special cases on p. 344 and in the problems. Before doing this it will be worthwhile to develop an alternate receiver realization for the case in which $\Lambda_m = 0$. In many cases this alternate realization will be more convenient to implement.

Matched Filter-Envelope Detector Realization. When $\Lambda_m = 0$, we must find $\sqrt{L_c^2 + L_s^2}$. We can do so by using a bandpass filter followed by an envelope detector, as shown in Fig. 4.57. Because $h(t)$ is the impulse response of a bandpass filter, it is convenient to write it as

$$h(t) = h_L(t) \cos [\omega_c t + \psi_L(t)], \tag{372}$$

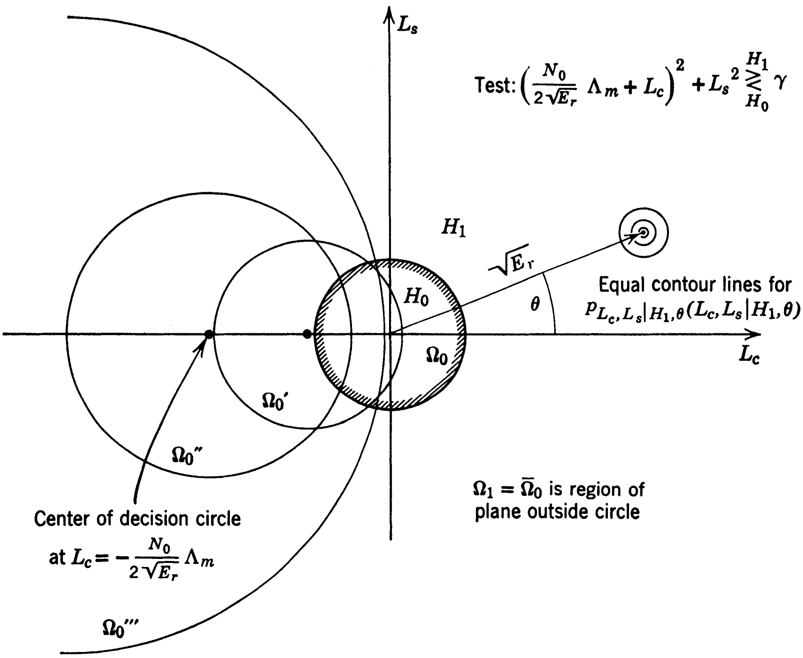

Fig. 4.56 Decision regions, partially coherent case.

where $h_L(t)$ and $\psi_L(t)$ are low-pass functions. The output at time T is

$$y(T) = \int_0^T h(T - \tau)\, r(\tau)\, d\tau. \tag{373}$$

Using (372), we can write this equation as

$$\begin{aligned} y(T) &= \int_0^T r(\tau)\, h_L(T - \tau) \cos[\omega_c(T - \tau) + \psi_L(T - \tau)]\, d\tau \\ &= \cos \omega_c T \int_0^T r(\tau)\, h_L(T - \tau) \cos[\omega_c\tau - \psi_L(T - \tau)]\, d\tau \\ &\quad + \sin \omega_c T \int_0^T r(\tau)\, h_L(T - \tau) \sin[\omega_c\tau - \psi_L(T - \tau)]\, d\tau. \end{aligned} \tag{374}$$

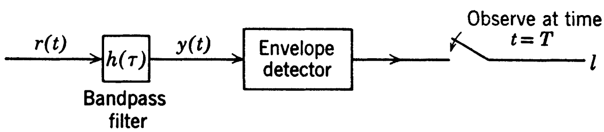

Fig. 4.57 Matched filter-envelope detector for uniform phase case.

This can be written as

$$y(T) \triangleq y_c(T)\cos\omega_c T + y_s(T)\sin\omega_c T$$
$$= \sqrt{y_c^2(T) + y_s^2(T)}\cos\left[\omega_c T - \tan^{-1}\frac{y_s(T)}{y_c(T)}\right]. \tag{375}$$

Observing that

$$y_c(T) = \mathrm{Re}\int_0^T r(\tau)\, h_L(T-\tau)\exp\left[+j\omega_c\tau - j\psi_L(T-\tau)\right] d\tau \tag{376a}$$

and

$$y_s(T) = \mathrm{Im}\int_0^T r(\tau)\, h_L(T-\tau)\exp\left[+j\omega_c\tau - j\psi_L(T-\tau)\right] d\tau, \tag{376b}$$

we see that the output of the envelope detector is

$$\sqrt{y_c^2(T) + y_s^2(T)} = \left|\int_0^T r(\tau)\, h_L(T-\tau)\exp\left[-j\psi_L(T-\tau) + j\omega_c\tau\right] d\tau\right|. \tag{377}$$

From (361) and (362) we see that the desired test statistic is

$$\sqrt{L_c^2 + L_s^2} = \left|\int_0^T r(\tau)\sqrt{2}\, f(\tau) e^{+j\phi(\tau)} e^{+j\omega_c\tau}\, d\tau\right|. \tag{378}$$

We see the two expressions will be identical if

$$h_L(T-\tau) = \sqrt{2}\, f(\tau) \tag{379}$$

and

$$\psi_L(T-\tau) = -\phi(\tau). \tag{380}$$

This bandpass matched filter provides a simpler realization for the *uniform* phase case.

The receiver in the uniform phase case is frequently called an incoherent receiver, but the terminology tends to be misleading. We see that the matched filter utilizes all the *internal* phase structure of the signal. The only thing missing is an *absolute* phase reference. The receiver for the known signal case is called a coherent receiver because it requires an oscillator at the receiver that is coherent with the transmitter oscillator. The general case developed in this section may be termed the partially coherent case.

To complete our discussion we consider the performance for some simple cases. There is no conceptual difficulty in evaluating the error probabilities but the resulting integrals often cannot be evaluated analytically. Because various modifications of this particular problem are frequently encountered in both radar and communications, a great deal of effort has been expended in finding convenient closed-form expressions and in numerical evaluations. We have chosen two typical examples to illustrate the techniques employed.

First we consider the radar problem defined at the beginning of this section (354–355).

Example 1 **(*Uniform Phase*).** Because this model corresponds to a radar problem, the uniform phase assumption is most realistic. To construct the ROC we must compute P_F and P_D. (Recall that P_F and P_D are the probabilities that we will exceed the threshold γ when noise only and signal plus noise are present, respectively.)

Looking at Fig. 4.55, we see that the test statistic is

$$l = L_c^2 + L_s^2, \tag{381}$$

where L_c and L_s are Gaussian random variables. The decision region is shown in Fig. 4.56. We can easily verify that

$$H_0: E(L_c) = E(L_s) = 0; \quad \operatorname{Var}(L_c) = \operatorname{Var}(L_s) = \frac{N_0}{2},$$

$$H_1: E(L_c|\theta) = \sqrt{E_r}\cos\theta; \quad E(L_s|\theta) = \sqrt{E_r}\sin\theta; \quad \operatorname{Var}(L_c) = \operatorname{Var}(L_s) = \frac{N_0}{2}. \tag{382}$$

Then

$$P_F \triangleq \Pr[l > \gamma|H_0] = \iint_{\Omega_0} \left(2\pi\frac{N_0}{2}\right)^{-1} \exp\left(-\frac{L_c^2 + L_s^2}{N_0}\right) dL_c\, dL_s. \tag{383}$$

Changing to polar coordinates and evaluating, we have

$$P_F = \exp\left(-\frac{\gamma}{N_0}\right). \tag{384}$$

Similarly, the probability of detection for a particular θ is

$$P_D(\theta) = \iint_{\Omega_0} \left(2\pi\frac{N_0}{2}\right)^{-1} \exp\left(-\frac{(L_c - \sqrt{E_r}\cos\theta)^2 + (L_s - \sqrt{E_r}\sin\theta)^2}{N_0}\right) dL_c\, dL_s. \tag{385}$$

Letting $L_c = R\cos\beta$, $L_s = R\sin\beta$, and performing the integration with respect to β, we obtain

$$P_D(\theta) = P_D = \int_{\sqrt{\gamma}}^{\infty} \frac{2}{N_0} R \exp\left(-\frac{R^2 + E_r}{N_0}\right) I_0\left(\frac{2R\sqrt{E_r}}{N_0}\right) dR. \tag{386}$$

As we expected, P_D does not depend on θ. We can normalize this expression by letting $z = \sqrt{2/N_0}\, R$. This gives

$$P_D = \int_{\sqrt{2\gamma/N_0}}^{\infty} z \exp\left(-\frac{z^2 + d^2}{2}\right) I_0(zd)\, dz, \tag{387}$$

where $d^2 \triangleq 2E_r/N_0$.

This integral cannot be evaluated analytically. It was first tabulated by Marcum [46, 48] in terms of a function commonly called Marcum's Q function:

$$Q(\alpha, \beta) \triangleq \int_{\beta}^{\infty} z \exp\left(-\frac{z^2 + \alpha^2}{2}\right) I_0(\alpha z)\, dz. \tag{388}$$

This function has been studied extensively and tabulated for various values of α, β (e.g., [48], [49], and [50]). Thus

$$P_D = Q\left(d, \left(\frac{2\gamma}{N_0}\right)^{1/2}\right). \tag{389}$$

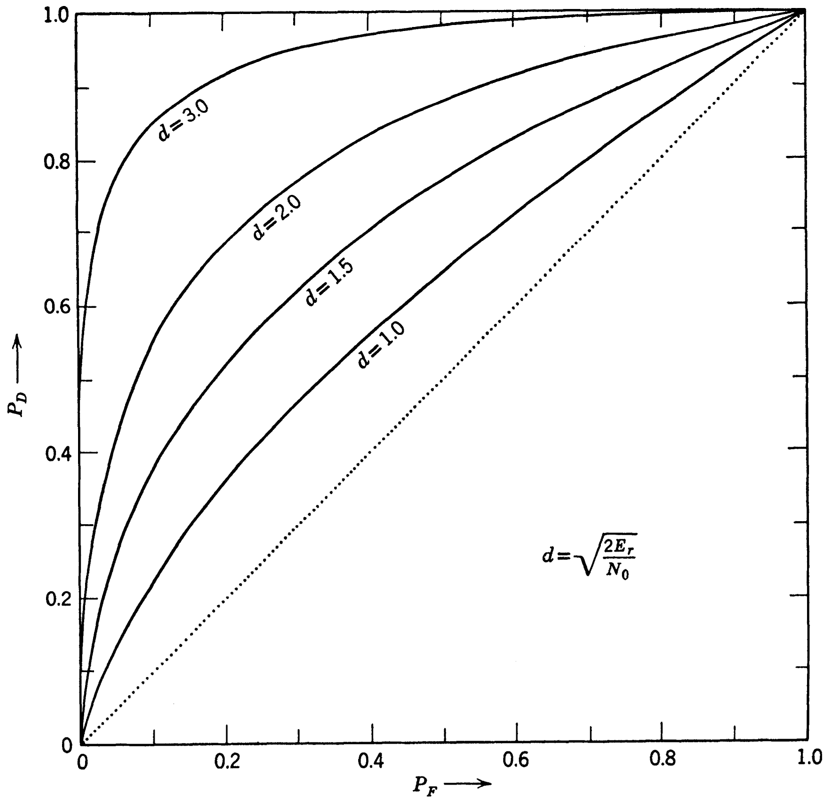

Fig. 4.58 Receiver operating characteristic, random phase with uniform density.

This can be written in terms of P_F. Using (384), we have

$$P_D = Q(d, \sqrt{-2 \ln P_F}). \tag{390}$$

The ROC is shown in Fig. 4.58. The results can also be plotted in the form of P_D versus d with P_F as a parameter. This is done in Fig. 4.59. Comparing Figs. 4.14 and 4.59, we see that a negligible increase of d is required to maintain the same P_D for a fixed P_F when we go from the known signal model to the uniform phase model for the parameter ranges shown in Fig. 4.59.

The second example of interest is a binary communication system in which some phase information is available.

Example 2. Partially Coherent Binary Communication. The criterion is minimum probability of error and the hypotheses are equally likely. We assume that the signals under the two hypotheses are

$$\begin{aligned} H_1\!: r(t) &= \sqrt{2E_r}\, f_1(t) \cos(\omega_c t + \theta) + w(t), \qquad 0 \le t \le T, \\ H_0\!: r(t) &= \sqrt{2E_r}\, f_0(t) \cos(\omega_c t + \theta) + w(t), \qquad 0 \le t \le T, \end{aligned} \tag{391}$$

where $f_0(t)$ and $f_1(t)$ are normalized and

$$\int_0^T f_0(t)\, f_1(t)\, dt = \rho; \qquad -1 \le \rho \le 1. \tag{392}$$

The noise spectral height is $N_0/2$ and $p_\theta(\theta)$ is given by (364). The likelihood ratio test is obtained by an obvious modification of the simple binary problem and the receiver structure is shown in Fig. 4.60.

We now look at Pr (ϵ) as a function of ρ, d^2, and Λ_m. Intuitively, we expect that as $\Lambda_m \to \infty$ we would approach the known signal problem, and $\rho = -1$ (the equal and opposite signals of (39)) would give the best result. On the other hand, as $\Lambda_m \to 0$,

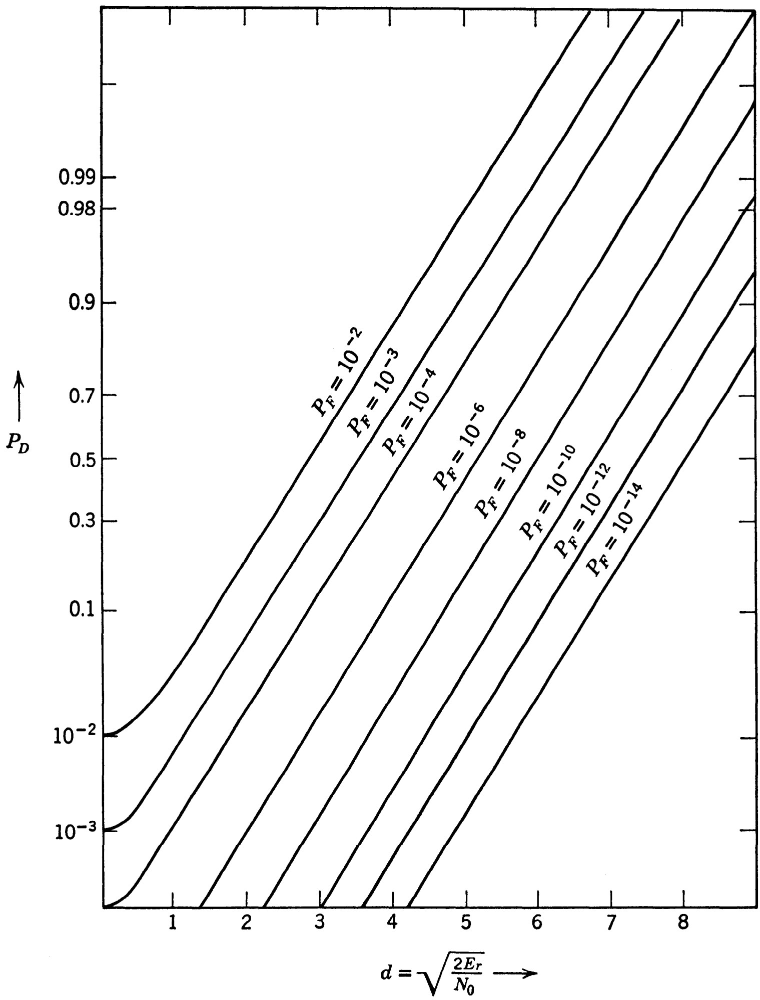

Fig. 4.59 Probability of detection vs d, uniform phase.

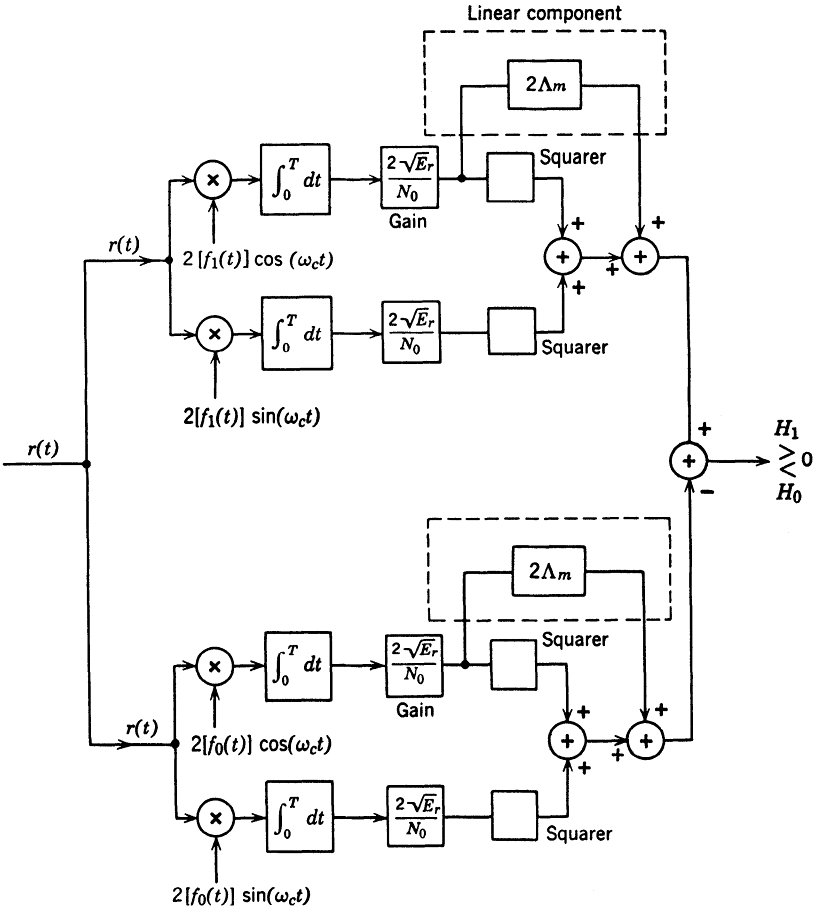

Fig. 4.60 Receiver: binary communication system.

the phase becomes uniform. Now, any correlation (+ or −) would move the signal points closer together. Thus, we expect that $\rho = 0$ would give the best performance. As we go from the first extreme to the second, the best value of ρ should move from -1 to 0.

We shall do only the details for the easy case in which $\rho = -1$; $\rho = 0$ is done in Problem 4.4.9. The error calculation for arbitrary ρ is done in [44].

When $\rho = -1$, we observe that the output of the square-law section is identical on both hypotheses. Thus the receiver is linear. The effect of the phase error is to rotate the signal points in the decision space as shown in Fig. 4.61.

Using the results of Section 4.2.1 (p. 257),

$$\Pr(\epsilon|\theta) = \int_{-\infty}^{0} \left(2\pi \frac{N_0}{2}\right)^{-1/2} \exp\left[-\frac{(x - \sqrt{E_r}\cos\theta)^2}{N_0}\right] dx \tag{393}$$

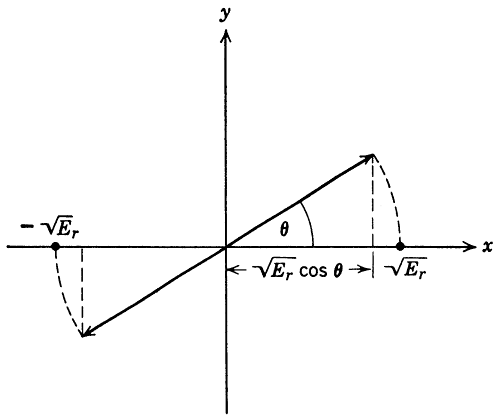

Fig. 4.61 Effect of phase errors in decision space.

or

$$\Pr(\epsilon|\theta) = \int_{-\infty}^{-\sqrt{2E_r/N_0}\cos\theta} \frac{1}{\sqrt{2\pi}} \exp\left(-\frac{z^2}{2}\right) dz. \tag{394}$$

Using (364),

$$\Pr(\epsilon) = \int_{-\pi}^{+\pi} \frac{\exp(\Lambda_m \cos\theta)}{2\pi I_0(\Lambda_m)} \Pr(\epsilon|\theta)\, d\theta. \tag{395}$$

This can be integrated numerically. The results for two particular values of d^2 are shown in Figs. 4.62 and 4.63.† The results for other ρ were also evaluated in [44] and are given in these figures. We see that for Λ_m greater than about 2 the negatively correlated signals become more efficient than orthogonal signals. For $\Lambda_m \geq 10$ the difference is significant. The physical significance of Λ_m will become clearer when we study phase estimating systems in Chapter II.2.

In this section we have studied a particular case of an unwanted parameter, a random phase angle. By using a family of densities we were able to demonstrate how to progress smoothly from the known signal case to the uniform phase case. The receiver consisted of a weighted sum of a linear operation and a quadratic operation. We observe that the specific receiver structure is due to the precise form of the density chosen. In many cases the probability density for the phase angle would not correspond to any of these densities. Intuitively we expect that the receiver developed here should be "almost" optimum for *any* single-peaked density with the same variance as the member of the family for which it was designed.

We now turn to a case of equal (or perhaps greater) importance in which both the amplitude and phase of the received signal vary.

† The values of d^2 were chosen to give a $\Pr(\epsilon) = 10^{-3}$ and 10^{-5}, respectively, at $\Lambda_m = \infty$.

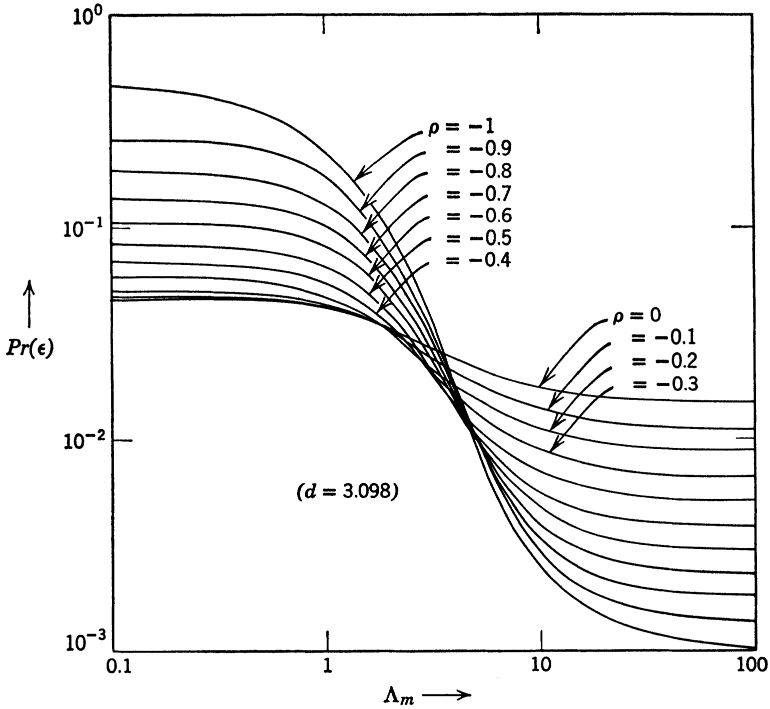

Fig. 4.62 Pr (ϵ), partially coherent binary system (10^{-3} asymptote) [44].

4.4.2 Random Amplitude and Phase

As we discussed in Section 4.1, there are cases in which both the amplitude and phase of the received signal vary. In the communication context this situation is encountered in ionospheric links operating above the maximum usable frequency (e.g., [51]) and in some tropospheric links (e.g., [52]). In the radar context it is encountered when the target's aspect or effective radar cross section changes from pulse to pulse (e.g., Swerling [53]).

Experimental results for a number of physical problems indicate that when the input is a sine wave, $\sqrt{2} \sin \omega_c t$, the output (in the absence of additive noise) is

$$r(t) = v_{ch}(t) \sin [\omega_c t + \theta_{ch}(t)]. \tag{396}$$

An exaggerated sketch is shown in Fig. 4.64*a*. The envelope and phase vary continuously. The envelope $v_{ch}(t)$ has the Rayleigh probability density shown in Fig. 4.64*b* and that the phase angle $\theta_{ch}(t)$ has a uniform density.

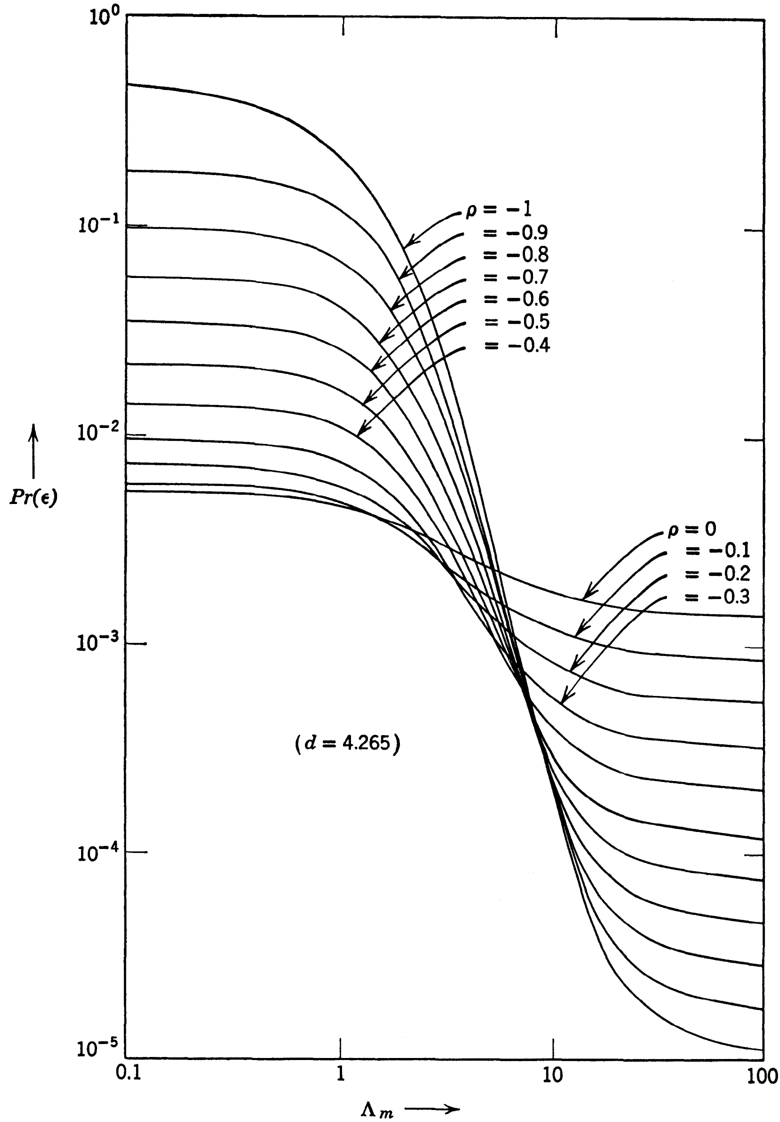

Fig. 4.63 Pr (ϵ), partially coherent binary system (10^{-5} asymptote) [44].

There are several ways to model this channel. The simplest technique is to replace the actual channel functions by piecewise constant functions (Fig. 4.65). This would be valid when the channel does not vary significantly

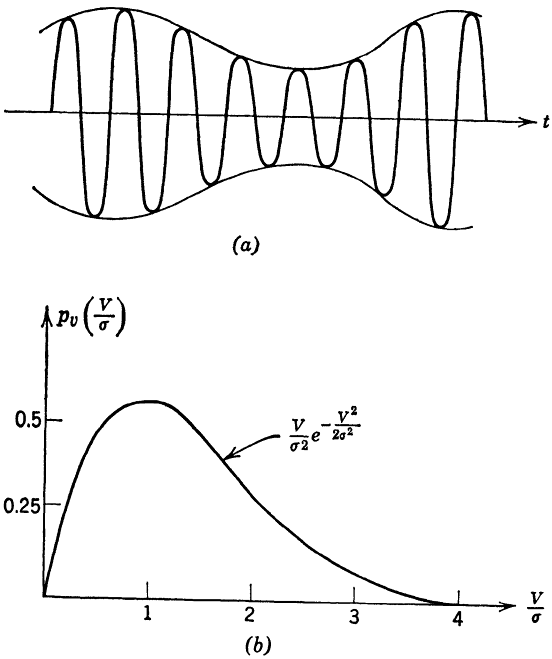

Fig. 4.64 Narrow-band process at output of channel, and the probability of its envelope.

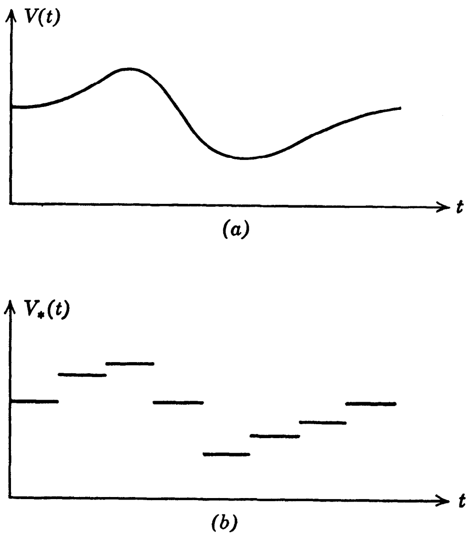

Fig. 4.65 Piecewise constant approximation: (*a*) actual envelope; (*b*) piecewise constant model.

in a T second interval. Given this "slow-fading" model, two choices are available. We can process each signaling interval independently or exploit the channel continuity by measuring the channel and using the measurements in the receiver. We now explore the first alternative.

For the simple binary detection problem in additive white Gaussian noise we may write the received signal under the two hypotheses as†

$$\begin{aligned} H_1 &: r(t) = v\sqrt{2}\, f(t) \cos[\omega_c t + \phi(t) + \theta] + w(t), \qquad 0 \le t \le T, \\ H_0 &: r(t) = w(t), \qquad 0 \le t \le T, \end{aligned} \tag{397}$$

where v is a Rayleigh random variable and θ is a uniform random variable.

We can write the signal component equally well in terms of its quadrature components:

$$\begin{aligned} \sqrt{2}\, v\, f(t) \cos[\omega_c t + \phi(t) + \theta] &= a_1\sqrt{2}\, f(t) \cos[\omega_c t + \phi(t)] \\ &\quad + a_2\sqrt{2}\, f(t) \sin[\omega_c t + \phi(t)], \\ &\qquad 0 \le t \le T, \end{aligned} \tag{398}$$

where a_1 and a_2 are independent zero-mean Gaussian random variables with variance σ^2 (where $E[v^2] = 2\sigma^2$; see pp. 158–161 of Davenport and Root [2]). We also observe that the two terms are *orthogonal*. Thus the signal out of a Rayleigh fading channel can be viewed as the sum of two orthogonal signals, each multiplied by an independent Gaussian random variable. This seems to be an easier way to look at the problem. As a matter of fact, it is just as easy to solve the more general problem in which the received waveform on H_1 is,

$$r(t) = \sum_{i=1}^{M} a_i\, s_i(t) + w(t), \qquad 0 \le t \le T, \tag{399}$$

where the a_i are independent, zero-mean Gaussian variables $N(0, \sigma_{a_i})$ and

$$\int_0^T s_i(t)\, s_j(t)\, dt = \delta_{ij}. \tag{400}$$

The likelihood ratio is

$$\Lambda[r(t)] = \underbrace{\int_{-\infty}^{\infty} \cdots \int_{-\infty}^{\infty}}_{M} p_{a_1}(A_1)\, p_{a_2}(A_2) \cdots p_{a_M}(A_M) \exp\left[+\frac{2}{N_0}\int_0^T r(t) \sum_{i=1}^{M} A_i s_i(t)\, dt - \frac{1}{N_0}\int_0^T \sum_{i=1}^{M}\sum_{j=1}^{M} A_i A_j\, s_i(t)\, s_j(t)\, dt\right] dA_1 \cdots dA_M. \tag{401}$$

† For simplicity we assume that the transmitted signal has unit energy and adjust the received energy by changing the characteristics of v.

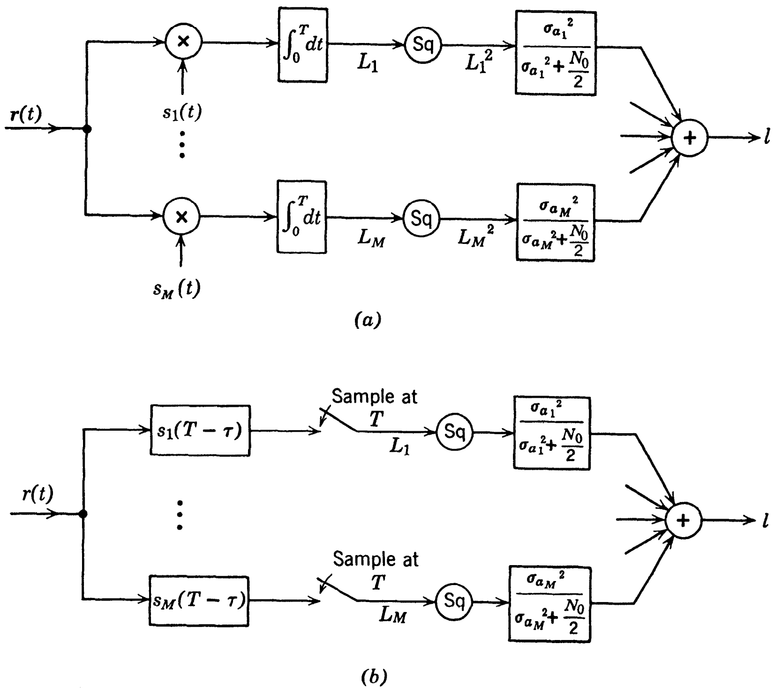

Fig. 4.66 Receivers for Gaussian amplitude signals: (*a*) correlation-squarer receiver; (*b*) filter-squarer receiver.

Defining

$$L_i = \int_0^T r(t)\, s_i(t)\, dt, \tag{402}$$

using the orthogonality of the $s_i(t)$, and completing the square in each of the M integrals, we find the test reduces to

$$l \triangleq \sum_{i=1}^{M} L_i^2 \left(\frac{\sigma_{a_i}^2}{\sigma_{a_i}^2 + N_0/2}\right) \underset{H_0}{\overset{H_1}{\gtrless}} \gamma. \qquad (403)\dagger$$

Two receivers corresponding to (403) and shown in Fig. 4.66 are commonly called a correlator-squarer receiver and a filter-squarer receiver, respectively. Equation 403 can be rewritten as

$$l = \sum_{i=1}^{M} L_i \left(\frac{\sigma_{a_i}^2 L_i}{\sigma_{a_i}^2 + N_0/2}\right) = \sum_{i=1}^{M} L_i \hat{a}_i. \tag{404}$$

† Note that we could have also obtained (403) by observing that the L_i are jointly Gaussian on both hypotheses and are sufficient statistics. Thus the results of Section 2.6 [specifically (2.326)] are directly applicable. Whenever the L_i have nonzero means or are correlated, the use of 2.326 is the simplest method (e.g., Problem 4.4.21).

This structure, shown in Fig. 4.67, can be interpreted as an estimator–correlator receiver (i.e., we are correlating $r(t)$ with our estimate of the received signal.) The identification of the term in braces as $\hat{a}_i$ follows from our estimation discussion in Section 4.2. It is both a minimum mean-square error estimate and a maximum a posteriori probability estimate. In Fig. 4.67*a* we show a practical implementation. The realization in Fig. 4.67*b* shows that we could actually obtain the estimate of the signal component as a waveform in the optimum receiver. This interpretation is quite important in later applications.

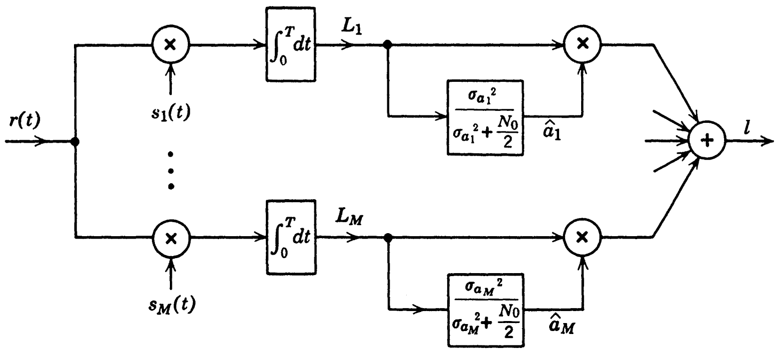

(*a*)

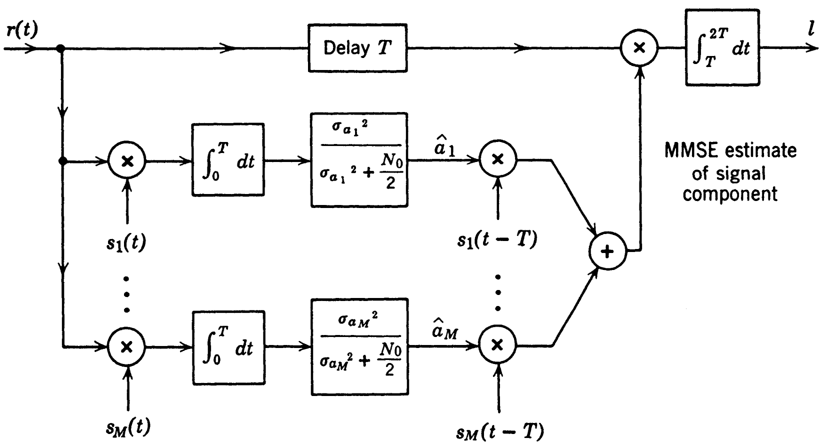

(*b*)

Fig. 4.67 Estimator-correlator receiver.

We now apply these results to the original problem in (397). If we relate L_1 to L_c and L_2 to L_s, we see that the receiver is

$$L_c^2 + L_s^2 \underset{H_0}{\overset{H_1}{\gtrless}} \gamma \tag{405}$$

(where L_c and L_s were defined in the random phase example). This can be realized, as shown in the preceding section, by a bandpass matched filter followed by an envelope detector. The two alternate receiver realizations are shown in Figs. 4.68*a* and *b*.

The next step is to evaluate the performance. We observe that L_c and L_s are Gaussian random variables with identical distributions. Thus the Rayleigh channel corresponds *exactly* to Example 2 on p. 41 of Chapter 2. In Equation (2.80), we showed that

$$P_D = (P_F)^{\sigma_0^2/\sigma_1^2}, \tag{2.80}$$

where σ_0^2 is the variance of L_c on H_0 and σ_1^2 is the variance of L_c on H_1. Looking at Fig. 4.58*a*, we see that

$$\sigma_0^2 = \frac{N_0}{2} \tag{406}$$

and

$$\sigma_1^2 = \frac{N_0}{2} + \sigma^2 E_t \triangleq \frac{N_0}{2} + \frac{\bar{E}_r}{2}, \tag{407}$$

where $\bar{E}_r \triangleq 2\sigma^2 E_t$ is the average received signal energy

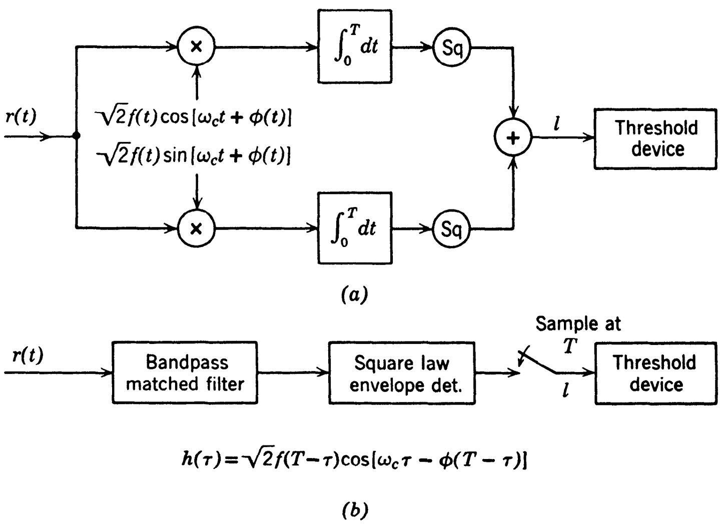

Fig. 4.68 Optimum receivers, Rayleigh channel: (*a*) squarer realization; (*b*) matched filter-envelope detector realization.

because v^2 is the received signal energy. Substituting (406) and (407) into (2.80), we obtain

$$P_F = (P_D)^{1 + \bar{E}_r/N_0} \tag{408}$$

The ROC is plotted in Fig. 4.69.

The solution to the analogous binary communication problem for arbitrary signals follows in a similar fashion (e.g., Masonson [55] and

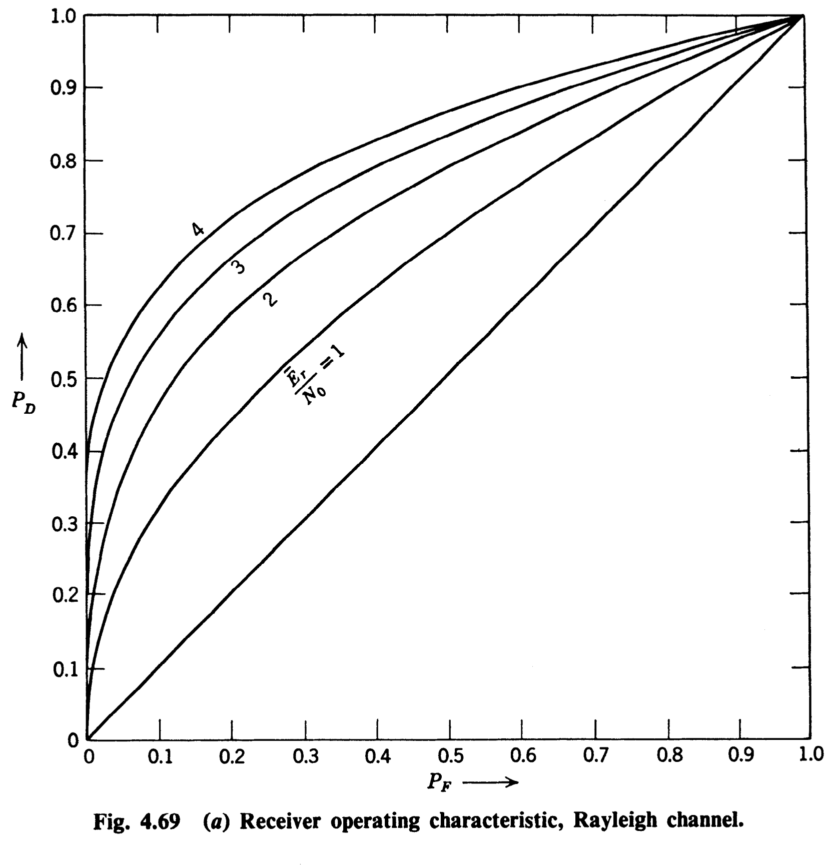

Fig. 4.69 (*a*) Receiver operating characteristic, Rayleigh channel.

Turin [56]). We discuss a typical system briefly. Recall that the phase angle θ has a uniform density. From our results in the preceding section (Figs. 4.62 and 4.63) we would expect that orthogonal signals would be optimum. We discuss briefly a simple FSK system using orthogonal signals. The received signals under the two hypotheses are

$$\begin{aligned} H_1: r(t) &= \sqrt{2}\, v\, f(t) \cos [\omega_1 t + \phi(t) + \theta] + w(t), \qquad 0 \le t \le T, \\ H_0: r(t) &= \sqrt{2}\, v\, f(t) \cos [\omega_0 t + \phi(t) + \theta] + w(t), \qquad 0 \le t \le T. \end{aligned} \tag{409}$$

The frequencies are separated enough to guarantee orthogonality. Assuming equal a priori probabilities and a minimum probability of error criterion, $\eta = 1$. The likelihood ratio test follows directly (see Problem 4.4.24).

$$L_{c1}^2 + L_{s1}^2 \underset{H_0}{\overset{H_1}{\gtrless}} L_{c0}^2 + L_{s0}^2. \tag{410}$$

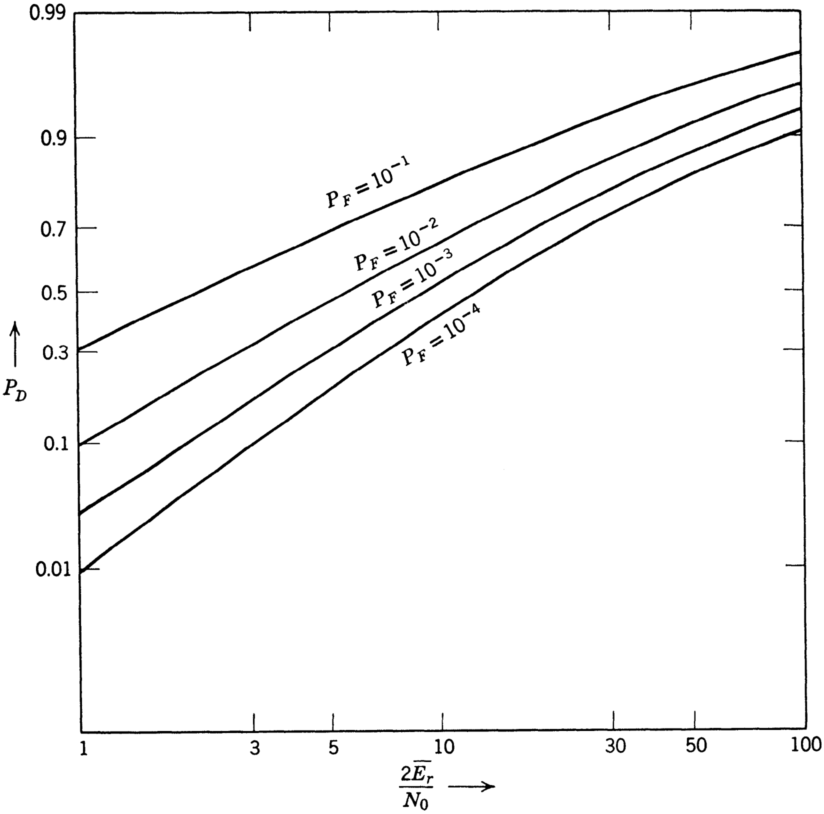

Fig. 4.69 (*b*) probability of detection vs. $2\bar{E}_r/N_0$.

The receiver structure is shown in Fig. 4.70. The probability of error can be evaluated analytically:

$$\Pr(\epsilon) = \frac{1}{2}\left[1 + \frac{1}{2}\frac{\bar{E}_r}{N_0}\right]^{-1}. \tag{411}$$

(See Problem 4.4.24.) In Fig. 4.71 we have plotted the $\Pr(\epsilon)$ as a function of $\bar{E}_r/N_0$. For purposes of comparison we have also shown the $\Pr(\epsilon)$ for

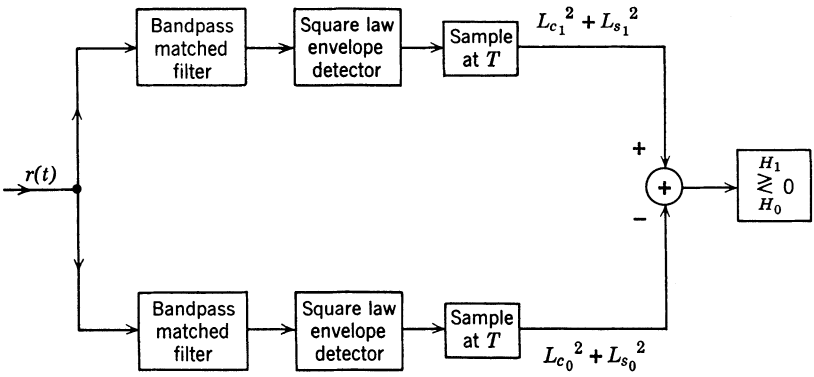

Fig. 4.70 Optimum receiver: binary communication system with orthogonal signals.

the known signal case and the uniform random phase case. We see that for both nonfading cases the probability of error decreases exponentially for large $\bar{E}_r/N_0$, whereas the fading case decreases only linearly. This is intuitively logical. Regardless of how large the average received energy becomes, during a deep signal fade the probability of error is equal or nearly equal to $\frac{1}{2}$. Even though this does not occur often, its occurrence keeps the probability of error from improving exponentially. In Chapter II.3 we shall find that by using diversity (for example, sending the signal over several independent Rayleigh channels in parallel) we can achieve an exponential decrease.

As we have already pointed out, an alternate approach is to measure the channel characteristics and use this measurement in the receiver structure. We can easily obtain an estimate of the possible improvement available by assuming that the channel measurement is *perfect*. If the measurement is perfect, we can use a coherent receiver. The resulting Pr (ϵ) is easy to evaluate. First we write the error probability conditioned on the channel variable v being equal to V. We then average over the Rayleigh density in Fig. 4.64*b*. Using coherent or known signal reception and orthogonal signals the probability of error for a given value V is given by (36) and (40),

$$\Pr(\epsilon|V) = \int_{V\sqrt{1/N_0}}^{\infty} \frac{1}{\sqrt{2\pi}} e^{-y^2/2}\, dy, \qquad (V \geq 0) \tag{412}$$

and

$$p_v(V) = \begin{cases} \dfrac{V}{\sigma^2} e^{-V^2/2\sigma^2}, & V \geq 0, \\ 0, & V < 0. \end{cases} \tag{413}$$

Thus

$$\Pr(\epsilon) = \int_0^\infty dV \frac{V}{\sigma^2} e^{-V^2/2\sigma^2} \int_{V\sqrt{1/N_0}}^\infty \frac{1}{\sqrt{2\pi}} e^{-y^2/2}\, dy. \tag{414}$$

Changing to polar coordinates and integrating, we obtain

$$\Pr(\epsilon) = \frac{1}{2}\left[1 - \left(\frac{\bar{E}_r/N_0}{1 + \bar{E}_r/N_0}\right)^{1/2}\right]. \tag{415}$$

The result is shown in Fig. 4.72.

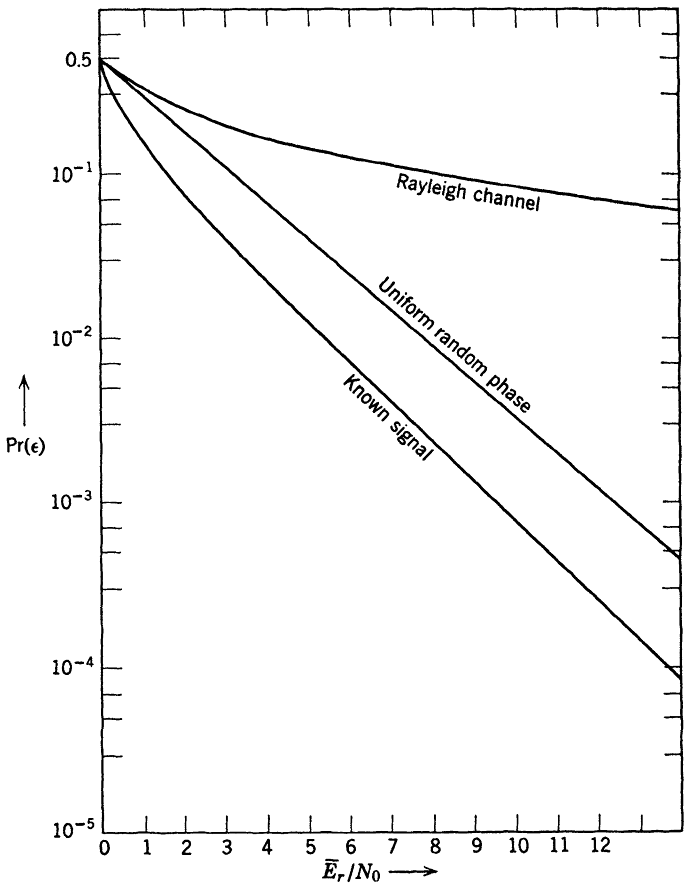

Fig. 4.71 Probability of error, binary orthogonal signals, Rayleigh channel.

Comparing (415) and (411) (or looking at Fig. 4.72), we see that perfect measurement gives about a 3-db improvement for high $\bar{E}_r/N_0$ values and orthogonal signals. In addition, if we measured the channel, we could use equal-and-opposite signals to obtain another 3 db.

Rician Channel In many physical channels there is a fixed (or "specular") component in addition to the Rayleigh component. A typical example is an ionospheric radio link operated below the maximum usable frequency (e.g., [57], [58], or [59]). Such channels are called Rician channels. We now illustrate the behavior of this type of channel for a

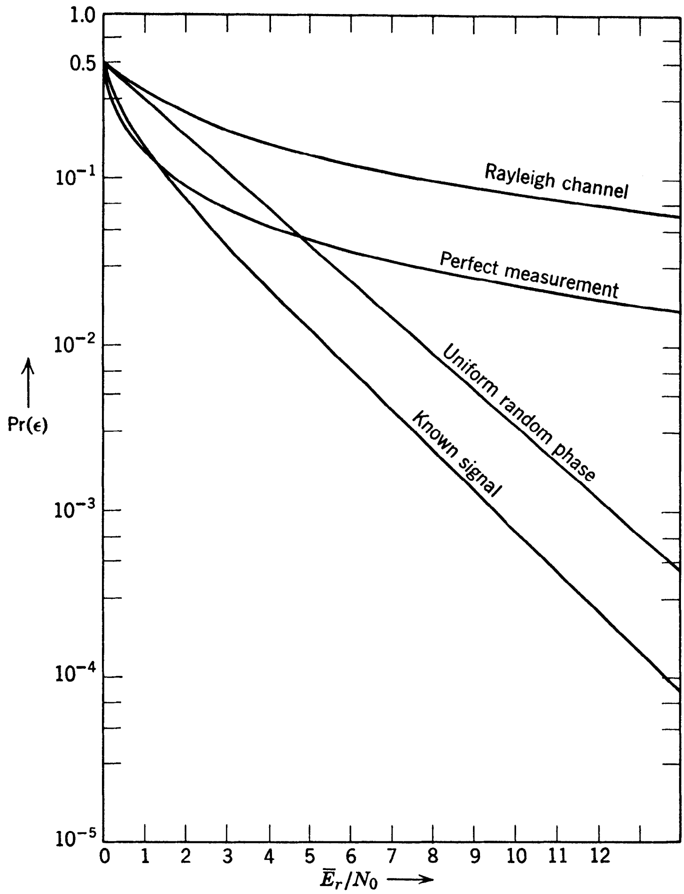

Fig. 4.72 Probability of error, Rayleigh channel with perfect measurement.

binary communication system, using orthogonal signals. The received signals on the two hypotheses are

$$
\begin{aligned}
H_1: r(t) &= \sqrt{2}\,\alpha\, f_1(t) \cos[\omega_c t + \phi_1(t) + \delta] \\
&\quad + \sqrt{2}\, v\, f_1(t) \cos[\omega_c t + \phi_1(t) + \theta] + w(t), \\
&\qquad\qquad\qquad\qquad 0 \le t \le T, \\
H_0: r(t) &= \sqrt{2}\,\alpha\, f_0(t) \cos[\omega_c t + \phi_0(t) + \delta] \\
&\quad + \sqrt{2}\, v\, f_0(t) \cos[\omega_c t + \phi_0(t) + \theta] + w(t), \\
&\qquad\qquad\qquad\qquad 0 \le t \le T,
\end{aligned}
\tag{416}
$$

where α and δ are the amplitude and phase of the specular component. The transmitted signals are orthonormal. In the simplest case α and δ are assumed to be known (see Problem 4.5.26 for unknown δ). Under this assumption, with no loss in generality, we can let $\delta = 0$. We may now write the signal component on H_i as

$$
a_1\{\sqrt{2}\, f_i(t) \cos[\omega_c t + \phi_i(t)]\} + a_2\{\sqrt{2}\, f_i(t) \sin[\omega_c t + \phi_i(t)]\}, \qquad (i = 0, 1). \tag{417}
$$

Once again, a_1 and a_2 are independent Gaussian random variables:

$$
\begin{aligned}
E(a_1) &= \alpha, \qquad E(a_2) = 0, \\
\operatorname{Var}(a_1) &= \operatorname{Var}(a_2) = \sigma^2.
\end{aligned}
\tag{418}
$$

The expected value of the received energy in the signal component on either hypothesis is

$$
E(E_r) = 2\sigma^2 + \alpha^2 \triangleq \sigma^2(2 + \gamma^2). \tag{419}
$$

where γ^2 is twice the ratio of the energy in the specular component to the average energy in the random component.

If we denote the total received amplitude and phase angle as

$$
v' = \sqrt{a_1^{\,2} + a_2^{\,2}}, \qquad \theta' = \tan^{-1}\frac{a_2}{a_1}. \tag{420}
$$

The density of the normalized envelope ($V_n' = V/\sigma) p_{v_n'}(X)$ and the density of the phase angle $p_{\theta'}(\theta')$ are shown in Fig. 4.73 ([60] and [56]). As we would expect, the phase angle probability density becomes quite peaked as γ increases.

The receiver structure is obtained by a straightforward modification of (398) to (405). The likelihood ratio test is

$$
\left(\frac{\alpha}{2\sigma^2} + \frac{1}{N_0} L_{c1}\right)^2 + \left(\frac{1}{N_0} L_{s1}\right)^2 \underset{H_0}{\overset{H_1}{\gtrless}} \left(\frac{\alpha}{2\sigma^2} + \frac{1}{N_0} L_{c0}\right)^2 + \left(\frac{1}{N_0} L_{s0}\right)^2. \tag{421}
$$

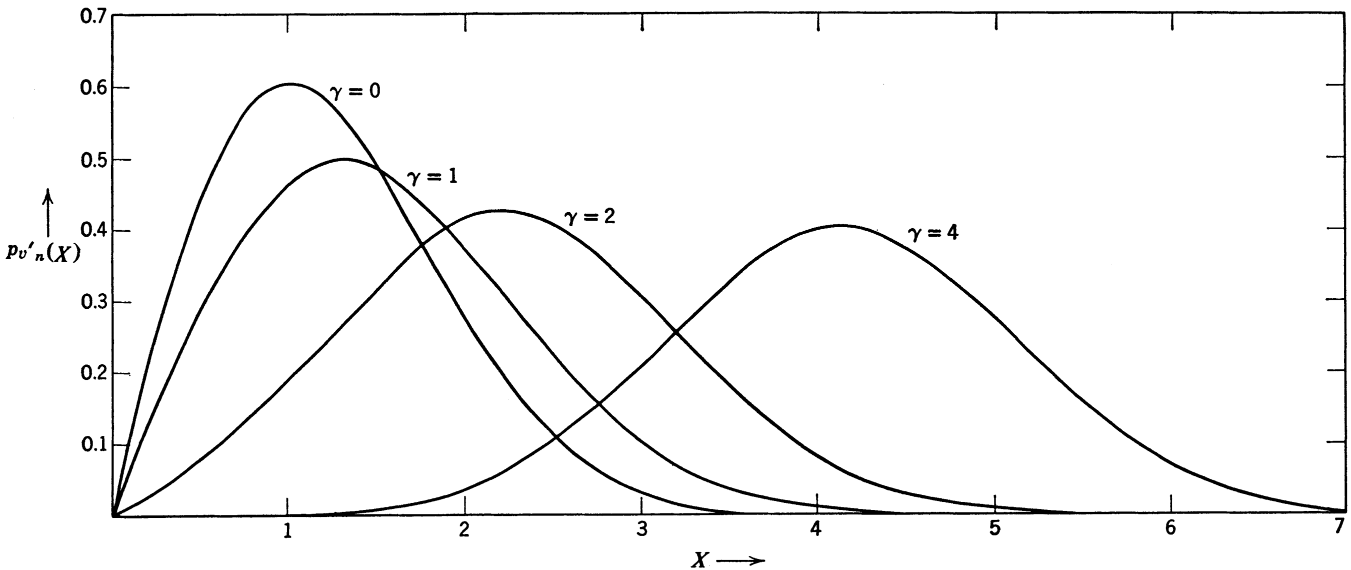

Fig. 4.73 (*a*) **Probability density for envelope, Rician channel.**

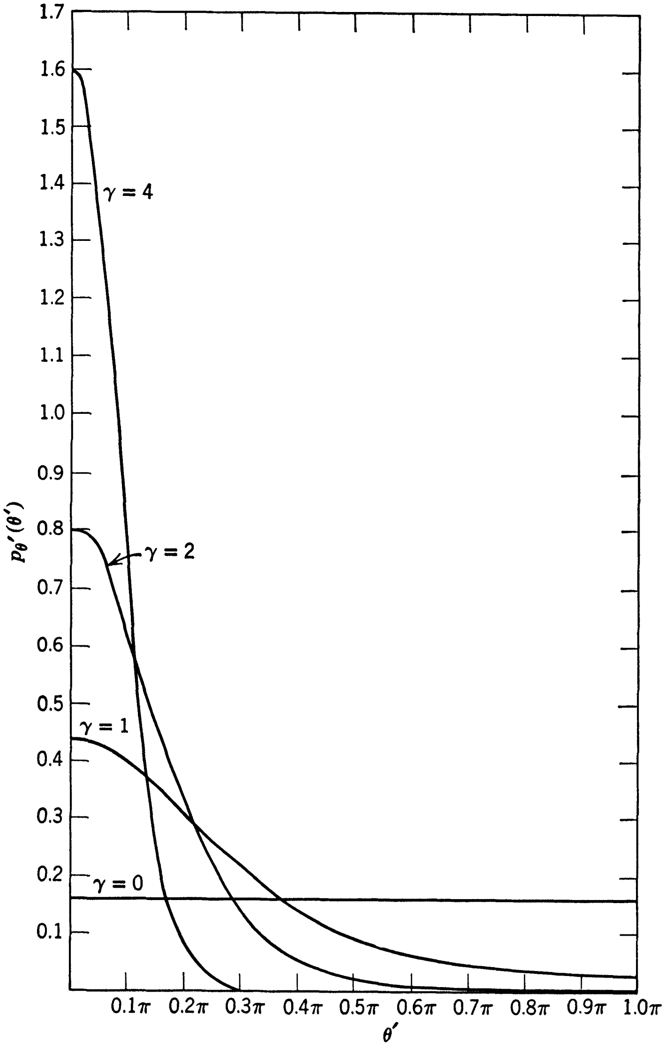

Fig. 4.73 (*b*) probability density for phase angle, Rician channel.

The receiver structure is shown in Fig. 4.74. The calculation of the error probability is tedious (e.g., [56]), but the result is

$$\Pr(\epsilon) = Q\left[\frac{\gamma}{(\beta + \frac{1}{2})^{1/2}\beta^{1/2}}, \frac{\gamma(\beta + 1)}{(\beta + 2)^{1/2}\beta^{1/2}}\right] - \left(\frac{\beta + 1}{\beta + 2}\right) \exp\left[-\frac{\gamma^2}{2}\left(\frac{\beta^2 + 2\beta + 2}{\beta^2 + 2\beta}\right)\right] I_0\left[\gamma^2 \frac{\beta + 1}{\beta(\beta + 2)}\right] \tag{422}$$

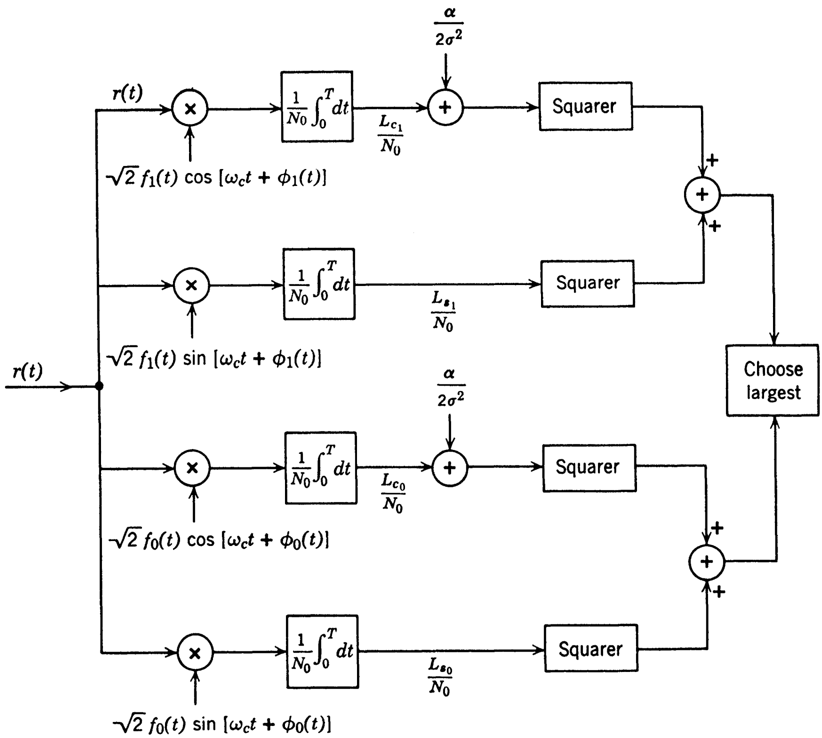

Fig. 4.74 Optimum receiver for binary communication over a Rician channel.

where $\beta \triangleq 2\sigma^2/N_0$ is the expected value of the received signal energy in the random component divided by N_0. The probability of error is plotted for typical values of γ in Fig. 4.75. Observe that $\gamma = 0$ is the Rayleigh channel and $\gamma = \infty$ is the completely known signal. We see that even when the power in the specular component is twice that of the random component the performance lies close to the Rayleigh channel performance. Once again, because the Rician channel is a channel of practical importance, considerable effort has been devoted to studying its error behavior under various conditions (e.g., [56]).

Summary As we would expect, the formulation for the M-ary signaling problem is straightforward. Probability of error calculations are once again involved (e.g., [61] or [15]). In Chapter II.3 we shall see that both the Rayleigh and Rician channels are special cases of the *general Gaussian* problem.

In this section we have studied in detail two important cases in which unwanted random parameters are contained in the signal components.

Because the probability density was known, the optimum test procedure followed directly from our general likelihood ratio formulation. The particular examples of densities we considered gave integrals that could be evaluated analytically and consequently led to explicit receiver structures. Even when we could not evaluate the integrals, the method of setting up the likelihood ratio was clear.

When the probability density of $\boldsymbol{\theta}$ is unknown, the best procedure is not obvious. There are two logical possibilities:

1. We can hypothesize a density and use it as if it were correct. We can investigate the dependence of the performance on the assumed density by using sensitivity analysis techniques analogous to those we have demonstrated for other problems.

2. We can use a minimax procedure. This is conceptually straightforward. For example, in a binary communication problem we find the

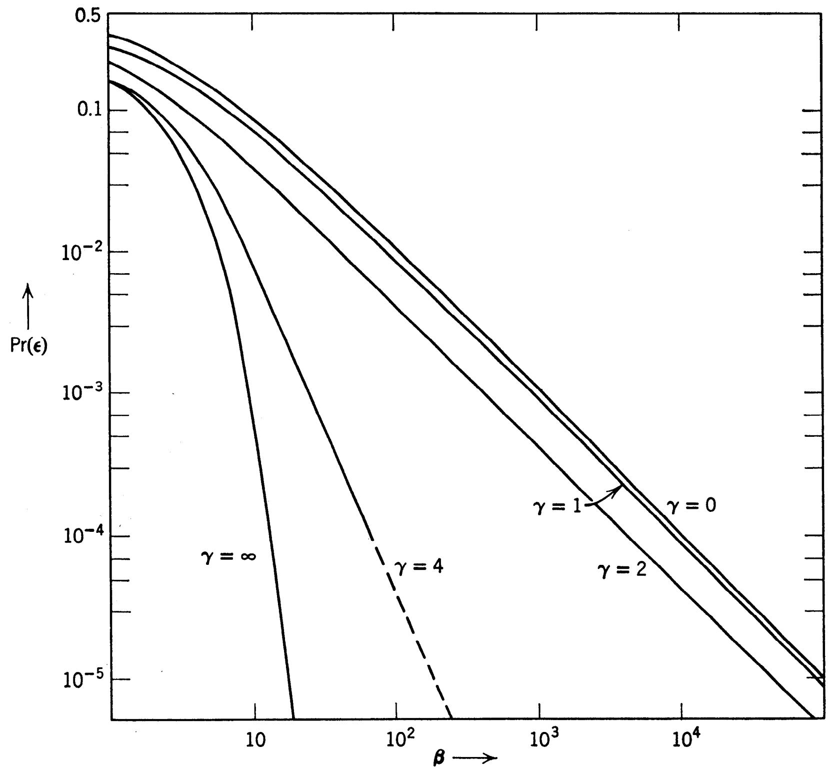

Fig. 4.75 Probability of error for binary orthogonal signals, Rician channel.

Pr (ϵ) as a function of $p_{\theta}(\boldsymbol{\theta})$ and then choose the $p_{\theta}(\boldsymbol{\theta})$ that maximizes Pr (ϵ) and design for this case. The two objections to this procedure are its difficulty and the conservative result.

The final possibility is for $\boldsymbol{\theta}$ to be a nonrandom variable. To deal with this problem we simply extend the composite hypothesis testing techniques that we developed in Section 2.5 to include waveform observations. The techniques are straightforward. Fortunately, in many cases of practical importance either a UMP test will exist or a generalized likelihood ratio test will give satisfactory results. Some interesting examples are discussed in the problems. Helstrom [14] discusses the application of generalized likelihood ratio tests to the radar problem of detecting signals of unknown arrival time.

4.5 MULTIPLE CHANNELS

In Chapter 3 we introduced the idea of a vector random process. We now want to solve the detection and estimation problems for the case in which the received waveform is a sample function from a vector random process.

In the simple binary detection problem, the received waveforms are

$$\begin{aligned} H_1&:\mathbf{r}(t) = \mathbf{s}(t) + \mathbf{n}(t), \qquad T_i \le t \le T_f, \\ H_0&:\mathbf{r}(t) = \mathbf{n}(t), \qquad T_i \le t \le T_f. \end{aligned} \tag{423}$$†

In the estimation case, the received waveform is

$$\mathbf{r}(t) = \mathbf{s}(t, A) + \mathbf{n}(t), \qquad T_i \le t \le T_f. \tag{424}$$

Two issues are involved in the vector case:

1. The first is a compact formulation of the problem. By using the vector Karhunen-Loéve expansion with scalar coefficients introduced in Chapter 3 we show that the construction of the likelihood ratio is a trivial extension of the scalar case. (This problem has been discussed in great detail by Wolf [63] and Thomas and Wong [64].)
2. The second is to study the performance of the resulting receiver structures to see whether problems appear that did *not* occur in the scalar case. We discuss only a few simple examples in this section. In Chapter II.5 we return to the multidimensional problem and investigate some of the interesting phenomena.

† In the scalar case we wrote the signal energy separately and worked with normalized waveforms. In the vector case this complicates the notation needlessly, and we use unnormalized waveforms.

4.5.1 Formulation

We assume that $\mathbf{s}(t)$ is a known vector signal. The additive noise $\mathbf{n}(t)$ is a sample function from an M-dimensional Gaussian random process. We assume that it contains a white noise component:

$$\mathbf{n}(t) = \mathbf{w}(t) + \mathbf{n}_c(t), \tag{425}$$

where

$$E[\mathbf{w}(t)\mathbf{w}^T(u)] = \frac{N_0}{2}\mathbf{I}\,\delta(t-u). \tag{426a}$$

a more general case is,

$$E[\mathbf{w}(t)\,\mathbf{w}^T(u)] = \mathbf{N}\,\delta(t-u). \tag{426b}$$

The matrix $\mathbf{N}$ contains only numbers. We assume that it is *positive-definite*. Physically this means that all components of $\mathbf{r}(t)$ or any linear transformation of $\mathbf{r}(t)$ will contain a white noise component. The general case is done in Problem 4.5.2. We consider the case described by (426*a*) in the text. The covariance function matrix of the colored noise is

$$E[\mathbf{n}_c(t)\,\mathbf{n}_c^T(u)] \triangleq \mathbf{K}_c(t, u). \tag{427}$$

We assume that each element in $\mathbf{K}_c(t, u)$ is square-integrable and that the white and colored components are independent. Using (425–427), we have

$$\mathbf{K}_{\mathbf{n}}(t, u) = \frac{N_0}{2}\mathbf{I}\,\delta(t-u) + \mathbf{K}_c(t, u). \tag{428}$$

To construct the likelihood ratio we proceed as in the scalar case. Under hypothesis H_1

$$\begin{aligned} r_i &\triangleq \int_{T_i}^{T_f} \mathbf{r}^T(t)\,\boldsymbol{\phi}_i(t)\,dt \\ &= \int_{T_i}^{T_f} \mathbf{s}^T(t)\,\boldsymbol{\phi}_i(t)\,dt + \int_{T_i}^{T_f} \mathbf{n}^T(t)\,\boldsymbol{\phi}_i(t)\,dt \\ &= s_i + n_i. \end{aligned} \tag{429}$$

Notice that all of the coefficients are scalars. Thus (180) is directly applicable:

$$\ln \Lambda[\mathbf{r}(t)] = \sum_{i=1}^{\infty} \frac{R_i s_i}{\lambda_i} - \frac{1}{2}\sum_{i=1}^{\infty}\frac{s_i^2}{\lambda_i}. \tag{430}$$

Substituting (429) into (430), we have

$$\begin{aligned} \ln \Lambda[\mathbf{r}(t)] &= \iint_{T_i}^{T_f} \mathbf{r}^T(t) \sum_{i=1}^{\infty} \frac{\boldsymbol{\phi}_i(t)\,\boldsymbol{\phi}_i^T(u)}{\lambda_i}\,\mathbf{s}(u)\,dt\,du \\ &\quad - \tfrac{1}{2}\iint_{T_i}^{T_f} \mathbf{s}^T(t) \sum_{i=1}^{\infty} \frac{\boldsymbol{\phi}_i(t)\,\boldsymbol{\phi}_i^T(u)}{\lambda_i}\,\mathbf{s}(u)\,dt\,du. \end{aligned} \tag{431}$$

Defining

$$\mathbf{Q_n}(t, u) = \sum_{i=1}^{\infty} \frac{\boldsymbol{\phi}_i(t)\, \boldsymbol{\phi}_i^T(u)}{\lambda_i}, \qquad T_i < t, u < T_f, \tag{432}$$

we have

$$\ln \Lambda[\mathbf{r}(t)] = \iint_{T_i}^{T_f} \mathbf{r}^T(t)\, \mathbf{Q_n}(t, u)\, \mathbf{s}(u)\, dt\, du - \frac{1}{2} \iint_{T_i}^{T_f} \mathbf{s}^T(t)\, \mathbf{Q_n}(t, u)\, \mathbf{s}(u)\, dt\, du. \tag{433}$$

Using the vector form of Mercer's theorem (2.253) and (432), we observe that

$$\boxed{\int_{T_i}^{T_f} \mathbf{K_n}(t, u)\, \mathbf{Q_n}(u, z)\, du = \delta(t - z)\mathbf{I}, \qquad T_i < t, z < T_f.} \tag{434}$$

By analogy with the scalar case we write

$$\mathbf{Q_n}(t, u) = \frac{2}{N_0}\, \mathbf{I}[\delta(t - u) - \mathbf{h}_o(t, u)] \tag{435}$$

and show that $\mathbf{h}_o(t, u)$ can be represented by a convergent series. The details are in Problems 4.5.1. As in the scalar case, we simplify (433) by defining,

$$\boxed{\mathbf{g}(t) = \int_{T_i}^{T_f} \mathbf{Q_n}(t, u)\, \mathbf{s}(u)\, du, \qquad T_i < t < T_f.} \tag{436}$$

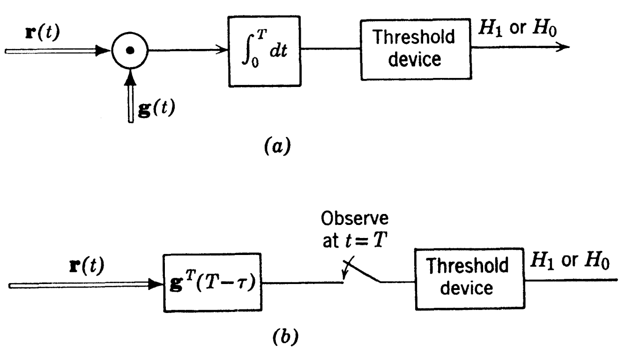

Fig. 4.76 Vector receivers: (*a*) matrix correlator; (*b*) matrix matched filter.

The optimum receiver is just a vector correlator or vector matched filter, as shown in Fig. 4.76. The double lines indicate vector operations and the symbol $\odot$ denotes the dot product of the two input vectors. We can show that the performance index is

$$
\begin{aligned}
d^2 &= \iint_{T_i}^{T_f} \mathbf{s}^T(t)\, \mathbf{Q_n}(t, u)\, \mathbf{s}(u)\, dt\, du \\
&= \int_{T_i}^{T_f} \mathbf{s}^T(t)\, \mathbf{g}(t)\, dt.
\end{aligned} \tag{437}
$$

4.5.2 Application

Consider a simple example.

Example.

$$
\mathbf{s}(t) = \begin{bmatrix} \sqrt{E_1}\, s_1(t) \\ \sqrt{E_2}\, s_2(t) \\ \vdots \\ \sqrt{E_M}\, s_M(t) \end{bmatrix}, \qquad 0 \le t \le T, \tag{438}
$$

where the $s_i(t)$ are orthonormal.

Assume that the channel noises are independent and white:

$$
E[\mathbf{w}(t)\mathbf{w}^T(u)] = \begin{bmatrix} \frac{N_0}{2} & & & 0 \\ & \frac{N_0}{2} & & \\ & & \ddots & \\ 0 & & & \frac{N_0}{2} \end{bmatrix} \delta(t - u). \tag{439}
$$

Then

$$
\mathbf{g}(t) = \begin{bmatrix} \dfrac{2\sqrt{E_1}}{N_0}\, s_1(t) \\ \vdots \\ \dfrac{2\sqrt{E_M}}{N_0}\, s_M(t) \end{bmatrix}. \tag{440}
$$

The resulting receiver is the vector correlator shown in Fig. 4.77 and the performance index is

$$
d^2 = \sum_{i=1}^{M} \frac{2E_i}{N_0}. \tag{441}
$$

This receiver is commonly called a maximal ratio combiner [65] because the inputs are weighted to maximize the output signal-to-noise ratio. The appropriate combiners for colored noise are developed in the problems.

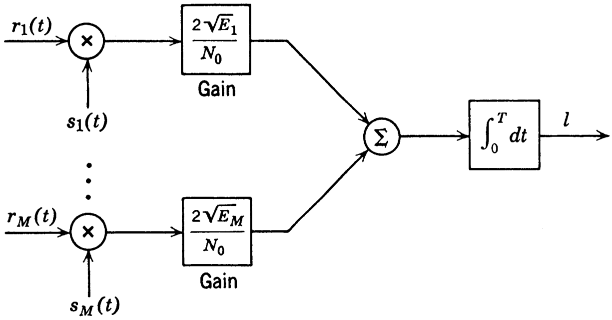

Fig. 4.77 Maximal ratio combiner.

Most of the techniques of the scalar case carry over directly to the vector case at the expense of algebraic complexity. Some of them are illustrated in the problems and a more detailed discussion is contained in Chapter II.5. The modifications for linear and nonlinear estimation are straightforward (see Problems 4.5.4 and 4.5.5). The modifications for unwanted parameters can also be extended to the vector case. The formulation for M channels of the random phase, Rayleigh, and Rician types is carried out in the problems.

4.6 MULTIPLE PARAMETER ESTIMATION

In this section we consider the problem of estimating a finite set of parameters, $a_1, a_2, \ldots, a_m$. We denote the parameters by the vector $\mathbf{a}$. We will consider only the additive white noise channel. The results are obtained by combining the classical multiple parameter estimation result of Chapter 2 with those of Section 4.2.

Our motivation for studying this problem is twofold:

1. One obvious reason is that multiple parameter problems are present in many physical situations of interest. A common example in radar is finding the range and velocity of a target by estimating the delay and Doppler shift of the returned pulse.

2. The second reason is less obvious. In Chapter 5 we shall consider the estimation of a continuous waveform, and we shall see that by expanding the waveform in a series we can estimate the coefficients of the series and use them to construct a waveform estimate. Thus the multiple parameter problem serves as a method of transition from single parameter estimation to waveform estimation.

4.6.1 Additive White Gaussian Noise Channel

Joint MAP Estimates. We assume that the signal depends on the parameter values $A_1, A_2, \ldots, A_M$. Then, for the additive channel, we may write the received signal as

$$r(t) = s(t, \mathbf{A}) + w(t), \qquad T_i \le t \le T_f, \tag{442}$$

where the $\mathbf{A}$ is a column matrix:

$$\mathbf{A} = \begin{bmatrix} A_1 \\ \vdots \\ A_M \end{bmatrix}. \tag{443}$$

We want to form the a posteriori density in terms of a suitable set of observables which we denote by the K-dimensional vector $\mathbf{r}$. We then find the estimate $\hat{\mathbf{a}}$ that maximizes the a posteriori density and let $K \to \infty$ to get the desired result.

The parameters $a_1, a_2, \ldots, a_M$ can be coupled either in the signal structure or because of an a priori statistical dependence. We can categorize this statistical dependence in the following way:

1. The $a_1, a_2, \ldots, a_M$ are *jointly Gaussian.*
2. The $a_1, a_2, \ldots, a_M$ are statistically independent and Gaussian.
3. The $a_1, a_2, \ldots, a_M$ are statistically independent but *not* Gaussian.
4. The $a_1, a_2, \ldots, a_M$ are not statistically independent and are *not* jointly Gaussian.

Our first observation is that Case 1 can be transformed into Case 2. The following property was proved in Chapter 2 (2.237).

Property. If $\mathbf{b}$ is a nonsingular linear transformation on $\mathbf{a}$ (i.e., $\mathbf{b} = \mathbf{L}\mathbf{a}$), then

$$\hat{\mathbf{b}}_{\text{map}} = \mathbf{L}\hat{\mathbf{a}}_{\text{map}},$$

and

$$\hat{\mathbf{a}}_{\text{map}} = \mathbf{L}^{-1}\hat{\mathbf{b}}_{\text{map}}. \tag{444}$$

We know that there is a nonsingular linear transformation that transforms any set of dependent Gaussian variables into a set of independent Gaussian variables (Chapter 2, pp. 101–105). Thus, if the a_i are dependent, we can estimate the b_i instead. Therefore the assumption

$$p_{\mathbf{a}}(\mathbf{A}) \triangleq p_{a_1 a_2 \cdots a_M}(A_1, \ldots, A_M) = \prod_{i=1}^{M} p_{a_i}(A_i) \tag{445}$$

effectively includes Cases 1, 2, and 3. Case 4 is much more involved in detail (but not in concept) and is of no importance in the sequel. We do not consider it here.

Assuming that the noise is white and that (445) holds, it follows in the same manner as the scalar case that the MAP estimates are solutions to the following set of M simultaneous equations:

$$0 = \left\{\frac{2}{N_0} \int_{T_i}^{T_f} \frac{\partial s(t, \mathbf{A})}{\partial A_i} [r(t) - s(t, \mathbf{A})]\, dt + \frac{\partial \ln p_{a_i}(A_i)}{\partial A_i}\right\}\Bigg|_{\mathbf{A} = \hat{\mathbf{a}}_{\text{map}}},$$

$$(i = 1, 2, \ldots, M). \tag{446}$$

If the a_i are Gaussian with zero-mean and variances $\sigma_{a_i}^2$, the equations reduce to a simple form:

$$\hat{a}_i = \frac{2\sigma_{a_i}^2}{N_0} \int_{T_i}^{T_f} \frac{\partial s(t, \mathbf{A})}{\partial A_i} [r(t) - s(t, \mathbf{A})]\, dt\Bigg|_{\mathbf{A} = \hat{\mathbf{a}}_{\text{map}}}, \qquad (i = 1, 2, \ldots, M). \tag{447}$$

This set of simultaneous equations imposes a set of *necessary* conditions on the MAP estimates. (We assume that the maximum is interior to the allowed region of $\mathbf{A}$ and that the indicated derivatives exist at the maximum.)

The second result of interest is the bound matrix. From Section 2.4.3 we know that the first step is to find the information matrix. From Equation 2.289

$$\mathbf{J}_T = \mathbf{J}_D + \mathbf{J}_P, \tag{448}$$

$$\mathbf{J}_{D_{ij}} = -E\left(\frac{\partial^2 \ln \Lambda(\mathbf{A})}{\partial A_i\, \partial A_j}\right), \tag{449}$$

and for a Gaussian a priori density

$$\mathbf{J}_P = \mathbf{\Lambda}_{\mathbf{a}}^{-1}, \tag{450}$$

where $\mathbf{\Lambda}_{\mathbf{a}}$ is the covariance matrix. The term in (449) is analogous to (104) in Section 4.2. Thus it follows easily that (449) reduces to,

$$\mathbf{J}_{D_{ij}} = \frac{2}{N_0} E_{\mathbf{a}}\left[\int_{T_i}^{T_f} \frac{\partial s(t, \mathbf{A})}{\partial A_i} \frac{\partial s(t, \mathbf{A})}{\partial A_j}\, dt\right]. \tag{451}$$

We recall that this is a bound with respect to the correlation matrix $\mathbf{R}_\epsilon$ in the sense that

$$\mathbf{J}_T - \mathbf{R}_\epsilon^{-1} \tag{452}$$

is nonnegative definite. If the a posteriori density is Gaussian, $\mathbf{R}_\epsilon^{-1} = \mathbf{J}_T$.

A similar result is obtained for unbiased estimates of nonrandom variables by letting $\mathbf{J}_P = \mathbf{0}$. The conditions for the existence of an efficient estimate carry over directly. Equality will hold for the ith parameter if and only if

$$\hat{a}_i[r(t)] - A_i = \sum_{j=1}^{K} k_j(\mathbf{A}) \int_{T_i}^{T_f} [r(t) - s(t, \mathbf{A})] \frac{\partial s(t, \mathbf{A})}{\partial A_j}\, dt. \tag{453}$$

To illustrate the application of this result we consider a simple example.

Example. Suppose we simultaneously amplitude- and frequency-modulate a sinusoid with two independent Gaussian parameters a, $N(0, \sigma_a)$, and b, $N(0, \sigma_b)$. Then

$$r(t) = s(t, A, B) + w(t) = \left(\frac{2E}{T}\right)^{1/2} B \sin(\omega_c t + \beta A t) + w(t); \qquad -\frac{T}{2} \le t \le \frac{T}{2}. \tag{454}$$

The likelihood function is

$$\ln \Lambda[r(t)|A, B] = \frac{1}{N_0} \int_{-T/2}^{T/2} \left[2r(t) - \left(\frac{2E}{T}\right)^{1/2} B \sin(\omega_c t + \beta A t)\right] \times \left(\frac{2E}{T}\right)^{1/2} B \sin(\omega_c t + \beta A t)\, dt. \tag{455}$$

Then

$$\frac{\partial s(t, A, B)}{\partial A} = \left(\frac{2E}{T}\right)^{1/2} B\, \beta t \cos(\omega_c t + \beta A t) \tag{456}$$

and

$$\frac{\partial s(t, A, B)}{\partial B} = \left(\frac{2E}{T}\right)^{1/2} \sin(\omega_c t + \beta A t). \tag{457}$$

Because the variables are independent, $\mathbf{J}_P$ is diagonal.

The elements of $\mathbf{J}_T$ are

$$\begin{aligned} J_{11} &= \frac{2}{N_0} E_{a,b} \int_{-T/2}^{T/2} \frac{2E}{T} B^2 \beta^2 t^2 \cos^2(\omega_c t + \beta A t)\, dt + \frac{1}{\sigma_a^2} \\ &\cong \sigma_b^2 \frac{T^2}{12} \frac{2E}{N_0} \beta^2 + \frac{1}{\sigma_a^2}, \end{aligned} \tag{458}$$

$$J_{22} = \frac{2}{N_0} E_{a,b} \int_{-T/2}^{T/2} \frac{2E}{T} \sin^2(\omega_c t + \beta A t) + \frac{1}{\sigma_b^2} \cong \frac{2E}{N_0} + \frac{1}{\sigma_b^2}, \tag{459}$$

and

$$\begin{aligned} J_{12} &= \frac{2}{N_0} E_{a,b} \left[\int_{-T/2}^{T/2} \frac{\partial s(t, A, B)}{\partial A} \cdot \frac{\partial s(t, A, B)}{\partial B}\, dt\right] \\ &= \frac{2}{N_0} E_{a,b} \left[\int_{-T/2}^{T/2} \frac{2E}{T} B \beta t \sin(\omega_c t + \beta A t) \cos(\omega_c t + \beta A t)\, dt\right] \cong 0. \end{aligned} \tag{460}$$

Thus the $\mathbf{J}$ matrix is diagonal. This means that

$$E[(\hat{a} - a)^2] \ge \left(\frac{1}{\sigma_a^2} + \sigma_b^2 \frac{T^2}{12} \frac{2E}{N_0} \beta^2\right)^{-1} \tag{461}$$

and

$$E[(\hat{b} - b)^2] \ge \left(\frac{1}{\sigma_b^2} + \frac{2E}{N_0}\right)^{-1}. \tag{462}$$

Thus we observe that the *bounds* on the estimates of a and b are uncorrelated. We can show that for large E/N_0 the actual variances approach these bounds.

We can interpret this result in the following way. If, each time the experiment was conducted, the receiver were *given* the value of b, the performance in estimating a would not be improved over the case in which the receiver was required to estimate b (assuming large E/N_0).

We observe that there are two ways in which $\mathbf{J}_{12}$ can be zero. If

$$\int_{-T/2}^{T/2} \frac{\partial s(t, A, B)}{\partial A} \frac{\partial s(t, A, B)}{\partial B}\, dt = 0 \tag{463}$$

before the expectation is taken, it means that for any value of A or B the partial derivatives are orthogonal. This is required for ML estimates to be uncoupled.

Even if the left side of (463) were not zero, however, the value *after* taking the expectation might be zero, which gives uncoupled MAP estimates.

Several interesting examples of multiple parameter estimation are included in the problems.

4.6.2 Extensions

The results can be modified in a straightforward manner to include other cases of interest.

1. Nonrandom variables, ML estimation.
2. Additive colored noise.
3. Random phase channels.
4. Rayleigh and Rician channels.
5. Multiple received signals.

Some of these cases are considered in the problems. One that will be used in the sequel is the additive colored noise case, discussed in Problem 4.6.7. The results are obtained by an obvious modification of (447) which is suggested by (226).

$$\hat{a}_i = \sigma_{a_i}{}^2 \int_{T_i}^{T_f} \left.\frac{\partial s(z, \mathbf{A})}{\partial A_i}\right|_{\mathbf{A}=\hat{\mathbf{a}}_{\text{map}}} [r_g(z) - g(z)]\, dz, \qquad i = 1, 2, \dots, M, \tag{464}$$

where

$$r_g(z) - g(z) \triangleq \int_{T_i}^{T_f} Q_n(z, u)[r(u) - s(u, \hat{\mathbf{a}}_{\text{map}})]\, du, \qquad T_i \le z \le T_f. \tag{465}$$

4.7 SUMMARY AND OMISSIONS

4.7.1 Summary

In this chapter we have covered a wide range of problems. The central theme that related them was an additive Gaussian noise component. Using this theme as a starting point, we examined different types of problems and studied their solutions and the implications of these solutions. It turned out that the formal solution was the easiest part of the problem and that investigating the implications consumed most of our efforts. It is worthwhile to summarize some of the more general results.

The simplest detection problem was binary detection in the presence of white Gaussian noise. The optimum receiver could be realized as a matched filter or a correlation receiver. The performance depended only on the normalized distance between the two signal points in the decision